



TAMPERE UNIVERSITY OF TECHNOLOGY

Biomedical Department



UNIVERSITAT POLITÈCNICA DE CATALUNYA

Enginyeria Electrònica

MULTICHANNEL BIOIMPEDANCE MEASUREMENT

Master of Science Thesis

(PFC)

Autor: Javier Gracia Tabuenca

Examiner: Jari Hyttinen

Abstract

TAMPERE UNIVERSITY OF TECHNOLOGY

Master Degree in Electronic Engineering

GRACIA TABUENCA, JAVIER: Multichannel Bioimpedance Measurement

Master of Science Thesis 66 pages, 6 Appendix pages

May 2009

Major: Electronic Engineering

Examiner: Jari Hyttinen

Keywords: bioimpedance, multichannel, Amplitude Modulation, undersampling,

This thesis is a research about the possibility of measure bioimpedance simultaneously in different body locations. It first rises a theoretical study facing the problem as a classic multichannel communication system with share channel, analysing the software and hardware problems involved for all the possibilities. The more suitable configuration chosen is based on frequency multiplexation, it consists of injecting isolated sine waves with different frequencies for each channel and uses a bandpass filter to get only the required one. About the signal processing the best option found is to record the signal using undersampling techniques and implements the filter digitally. Moreover a three channel test device has been made following the calculations for a eight channels one, in order to test the theoretical research and to find possible practical limitations. Finally this test device has been used for a concrete purpose, the breathing measuring in three points on the thorax.

Table of Contents

Abstract.....	2
Abbreviations	5
1. Introduction.....	6
2. Background.....	7
2.1 Bioimpedance.....	7
2.1.1 Electronic model	7
2.1.2 Properties	8
2.2. Instrumentation.....	12
2.2.1 Biopotential Electrodes	12
2.2.2 tetrapolar.....	13
2.2.3 Electronic global model.....	14
2.2.4 Current Injector Properties.....	14
2.2.5 Howland improved circuit.....	16
2.2.6 Instrumentation Amplifier.....	18
2.3 Processing Background.....	19
2.3.1 Amplitude Modulation	19
2.4.2 Undersampling.....	21
3. Methods.....	25
3.1. Multichannel Bioimpedance System Approach	25
3.1.1 Time multiplexing	25
3.1.2 Frequency multiplexing	28
3.1.3 Conclusions.....	33
3.2. Prototype Device.....	34
3.2.1 Voltage to Current Converter	35
3.2.2 Instrumentation Amplifiers.....	37
3.2.3 Antialiasing filter	38
3.2.4 Processing.....	39
3.3. Calibration.....	41
3.3.1 Current source output impedance calibration	41
3.3.2 Gain calibration for a fix frequency.....	45
3.3.3 Frequencies dependence correction.....	46
3.3.4 Calibration Procedure.....	47
3.4. Test method	48
3.4.1 Processing Testing.....	48
3.4.2 Calibration Testing.....	48
3.4.3 Channel addition effects test.....	49
3.4.4 Complex Impedances Testing	50
3.4.5 On body testing.....	51
4. Results.....	53
4.1 Processing testing	53
4.2 Calibration Testing.....	54
4.2.1 Variable Gain Fix frequency	54
4.2.2 Variable Gain Variable Frequency	54

4.3 Channel addition test.....	56
4.3.1 Dynamic analysis.....	56
4.3.2 Static analysis.....	57
4.4 Complex Impedances	58
4.5 On body analysis.....	59
5. Conclusions.....	59
5.1 Achievements.....	59
5.2 Errors and Improvements.....	59
5.3 Future Work.....	60
References.....	62
Apendix A : Prototype Device Electronic Schematics.....	63

Abbreviations

AC	Alternating Current
ADC	Analog Digital Converter
AM	Amplitude Modulation
CMRR	Common-Mode Rejection Ratio
DC	Direct Current
DDS	Direct Digital Synthesis
FFT	Fast Fourier Transform
GIC	Generalized Impedance Converter
NIC	Negative Impedance Converter
OP-AMP	Operational Amplifier
SNR	Signal Noise Ratio

1. Introduction

As all the matter the human body has a number of electric features, the group of properties related with the opposition against an alternating current flow, are known as bioimpedance. The way to measure is not different from the conventional impedances measuring, which consists of supplying a small alternating current signal, and measuring the variations in the voltage, then the impedance is calculated with the amplitude and phase changes between the original signal and the recorded one.

The bioimpedance measuring provides a simple and non-invasive method to know the composition of the inside of the body. The estimation of this composition can be used in different ways to obtain information, on one hand a static version is used to determine the kind or quantity of a tissue, such as the amount of fat body, body hydration, or even to generate images for the most advanced applications as bioimpedance tomography. On the other hand the changes in the tissues are recorded along the time, to estimate biological signals related with this variations, for instance signals related with breathing or blood flow.

Usually the actual applications for the bioimpedance measurement are limited to being recorded in a single place, the possibility of having a simultaneous bioimpedance measuring would give the opportunity to obtain more information simultaneously. Hence this information could be used to improve the measurements by the comparison, for example removing an overlapped signal or artefacts, increasing the measuring area in big changes as the breathing, or just to measure independent signals.

This thesis presents a research for the problems involved in the addition of bioimpedance measurement in a same body. The thesis could be divided in three parts a theoretical study seeking all the possibilities and reasoning the most adequate choice, an implementation of the theory in a test device, and the use of this device for a concrete application, the breathing measuring.

The main problem in the measure points addition is the interference between the injected signals, the theoretical study analyses this problem as a classical multichannel communication problem, where in this case the body is the shared transmission channel. Under this view, to share the transmission channel the signals have to be multiplexing in the time or in the frequency domain.

The chosen options is the frequency multiplexing, which can be more complex but provides better flexibility and scalability and has the property of being able to read all the signals from all the points. Considering the high frequencies injected, the best solution found is to use undersampling techniques together with digital filtering and modulation, in order to reduce the processing resources, and improves the selection.

The test device is calculated for eight channels, nevertheless just three are physically implemented. To get a complete independence from the signals every channel is isolated. The current injector chosen is an Improved Howland with the output impedance trimmed manually for each channel.

Finally a body test is done to check the right working in practice, the test consist of measuring the breathing signal by recording the lungs resistance changes from different points in the thorax.

2. Background

2.1 Bioimpedance

As all the materials, organic tissues have a group of electrical properties. Bioimpedance refers to the opposition of the electric current flow through these organic tissues. A volume conductor conducts the electric current with finite impedance which depends on the material composition, in the organic tissues case this volume is not an homogeneous substance, it is a complex structure of different materials, compositions and layouts, it provides the biologic tissues a number of complex and special properties.

2.1.1 Electronic model

To begin to understand these features, it is necessary start by the basic piece of the organic tissues, the cell. Cells consist of a group of organelles floating in a dissolution enclosed within the plasma membrane. The impedances in these parts are different from each other. Specifically, plasma membrane is made of a lipids double layer with some embedded proteins, this structure acts as a capacitor with a resistivity around $100 \Omega/\text{cm}^2$ and a capacitance of $1\mu\text{F}/\text{cm}^2$. The internal fluid is an ionic dissolution hence the resistance is lower, about $100 \Omega/\text{cm}$. In addition, the current can flow through the external fluids, it has about $60 \Omega/\text{cm}$ [1]. All this information can be modelled as the below [figure](#) shows.

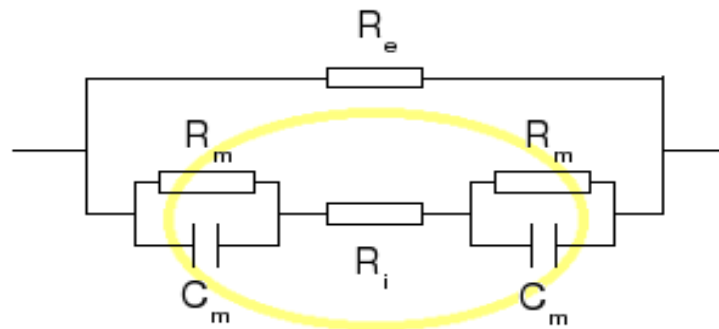


Figure 2.1. Electronic model of an individual cell. Where R_m and C_m represent the membrane impedance, R_e the external fluid resistance, and R_i the internal cell resistance. The yellow ellipse indicates the limit between the internal and external sides of the cell.

It is the model of a single cell, however the organic tissues are a collection of cells quite different in size and composition into an ionic salt dissolution. Anyhow even with these differences between cells, if this structure is kept current path through a tissue can be guess. It is easy to realise that this flow is heavily influenced by current frequency, in one hand the low frequencies piercing a tissue cannot cross the cellular

membrane capacitance, then these flow by the extracellular region. In the other hand when the frequency increases, the resistivity in the capacitances decreases leaving the current through the internal fluids.

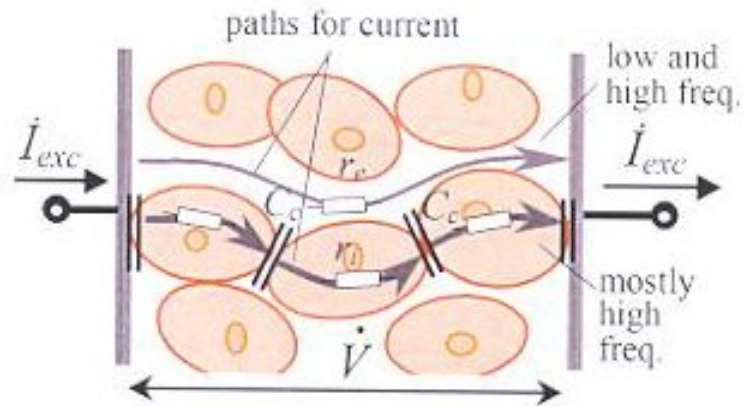


Figure 2.2. Comparison of the different paths follow by a current in an organic tissue depending on these frequencies. [2]

All this microscopic behaviour could be simplified using a macroscopic impedance model which reflects the external and internal resistance, and the membrane capacitance.

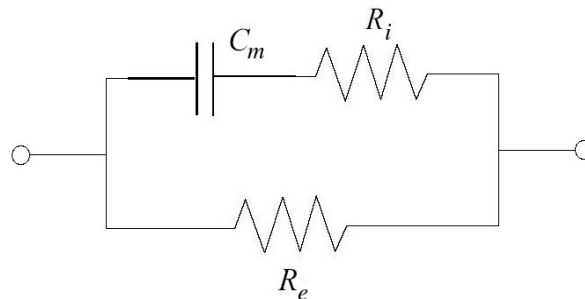


Figure 2.3. Simplified electronic model for organic tissue, R_e represents the external fluid resistance by the low frequency currents flow, and C_m with R_i , the path of the higher frequencies which have to thought the capacitance to pierce this branch. [3]

2.1.2 Properties

The model described in the previous section is a quite accurate model to represent the organic tissues, nevertheless it is not as simple as it looks, and because the value of the parts are affected by intrinsic and extrinsic factors. The main influential factors and its effects are discussed below:

- **Dissolution:** The electrical current in the tissues is an ionic current instead of a electric current, it means the carriers are the ions and not the electrons. Thus a variation in the ionic concentration affects the conductivity, this phenomenon is linked with the tissue hydration.

- **Current Frequency:** The special composition and distribution of the tissues produces that the permittivity changes with the current frequency injected. When an electric field is applied across a conducting medium dipole elements polarize in the field direction, if the field is alternating, the molecules polarize and depolarize according to the oscillation frequency. However if the frequency is high enough some molecules do not have time to come back to the depolarized state, staying permanently in a polarized position. The time needed to get depolarize is call *relaxation time*, and it depends on the molecule shape and composition, big complex molecules like proteins have low *relaxation times*, and simple molecules, such as water, have higher ones.

In a conductor with a mix of all range size molecules the polarization effect occurs at different frequencies. This and other phenomenons change the permittivity of the material depending on the frequency, this relation is charted in the Figure 2.4.

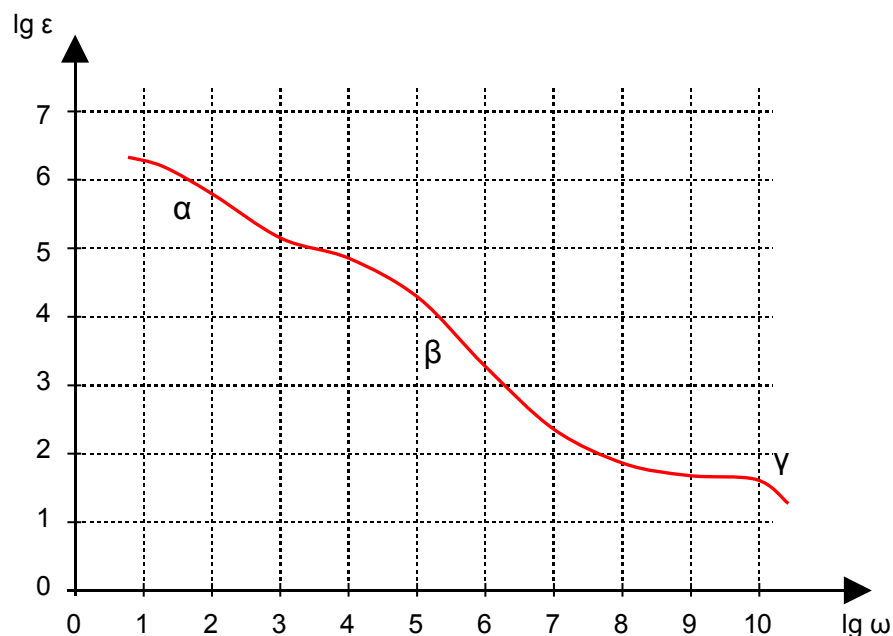


Figure 2.4. Relation between the frequency and permittivity. Abscissas axis belong to frequency in a logarithmic scale, ordinates axis shows the permittivity. Greek letters define the dispersion areas.[1]

Figure 2.4 shows the behaviour of the permittivity with the frequency increase, moreover three falls can be distinguished, these are called *dispersion regions* and have different reasons. The first one, the α -dispersion occurs at low frequencies, from 10 Hz to 10 kHz, and is owed to the ionic currents and the membrane polarization. B-dispersion happens in the 10kHz to 10MHz range because of the macromolecules relaxation such as the organelles and membrane proteins. Finally γ -dispersion appears in higher than 10MHz frequencies, caused by the water molecules relaxation.[5]

- **Temperature:** As in all the conductors the temperature increase makes easier the movement of the carriers, improving in this case the ionic current and reducing the *relaxation times*. It produces a decrement in the resistivity and an increment in the permittivity

$$\begin{aligned}\Delta\rho/\rho &= -1\% / ^\circ\text{C} \\ \Delta\varepsilon/\varepsilon &= +1.2\% / ^\circ\text{C} \quad \text{a 1 Mhz [1]}\end{aligned}$$

In the alive tissues the temperature usually is constant, however is a variable to bear in mind if the tissue suffers important temperature changes.

- **Anisotropy:** Some tissues, specially the striated muscles and bones exhibit a special behaviour called *anisotropy*. It means that a tissue or material has different physical properties in different directions.

For organic tissues *anisotropy* in impedance is due to the path followed by current flow. As illustrate the figure 2.5 the path of current is longer between points 1 and 2, than between 3 and 4. It is because of the inhomogeneous and rigid layout of the cells. For instance the resistivity of skeletal muscle is more that ten times higher in the longitudinal direction than in the transverse direction. [1]

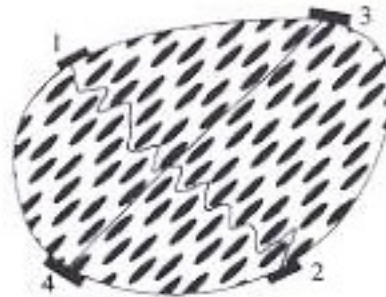


Figure 2.5. Impedance anisotropy in an organic tissue. The current path between the points 3-4 is smaller than in between 1-2.[3]

The behaviour under an injected current in all the organic tissues is the same, however each tissue has different thresholds depending on the kind, quantity, and cells layout. For instance on one hand, blood has a small number of cells floating in an ionic dissolution, thus the current flows better by the dissolution conferring it a low resistance, on the other, the bones are a collection of dry and fixed cells, and then the resistance becomes higher.

Table 1.1, shows typical resistivity values of tissues in low frequencies, it gives a first idea about difference between the tissues. [4]

Tissue	Resistivity
Plasma	60 $\Omega \cdot \text{cm}$
Blood	150 $\Omega \cdot \text{cm}$
Skeletal Muscle	125 $\Omega \cdot \text{cm}$ (long.) 1800 $\Omega \cdot \text{cm}$ (trans.)
Heart Muscle	160 $\Omega \cdot \text{cm}$ (long.) 424 $\Omega \cdot \text{cm}$ (trans.)
Nervous Tissue	580 $\Omega \cdot \text{cm}$
Lungs	727 $\Omega \cdot \text{cm}$ 2363 $\Omega \cdot \text{cm}$
Fat	2500 $\Omega \cdot \text{cm}$
Bones	16600 $\Omega \cdot \text{cm}$

A more accurate way to show the typical features of the tissues is by a chart that shows the conductivity and the permittivity of the material according to the frequency, these are known as *dielectric dispersion charts*. In Figure 2.6, a pair of this chart illustrates the differences between the skin and skeletal tissues.

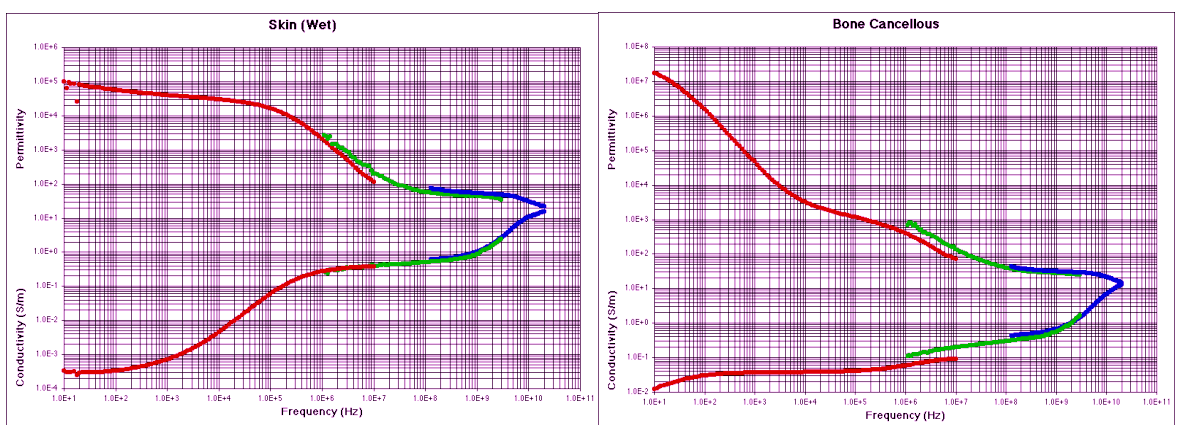


Figure 2.6. Comparison of the electrical properties in two different tissues using a dielectric dispersion chart. Left one bellows to wet skin where the conductivity and permittivity are high due to ions fluid and the right one to a bone. [4]

2.2. Instrumentation

The impedance in a volume is defined by the Ohm's law as:

$$\bar{Z} = \frac{\bar{V}}{\bar{I}} \quad (2.1)$$

Hence, an impedance value can be calculated in two ways, applying a known voltage and measuring the current flow, or injecting a known current and measuring the voltage. This section discusses the most common design electronic issues involved in bioimpedance measurement devices for the fix current option.

2.2.1 Biopotential Electrodes

The biopotential electrodes are the interface between the body and the electronic measuring device. This bridge is necessary because the currents flowing into the body are ionic currents whereas in the electronic device the current is led by electrons. Thus electrodes are transducers to turn an ionic current to an electric current.

The current conversion is based on a reduction-oxidation reaction. The electric current in the metal moves the electrons away from the metal surface this produces an oxidation reaction which generates cations, this cations are discharged (reduction reaction) in the electrolyte. The reaction involved in the anions is similar, in this case anions come to the electrode surface and are oxidized becoming neutrals and giving off some electrons to the electrode.

This is the current transfer working, however this reaction appears even without current, when a metal is immersed in an ionic solution containing ions of this metal, this ions turn cations, thus the solution to maintain neutrality of charge must be an equal number of anions. It generates disequilibrium of charge anions in the electrode surface which produces a potential difference known as *half-cell potential*. This phenomenon has a meaningful importance in the motion artefacts, because the movements reorder the ionic equilibrium changing the *half-cell potential*. [1]

Once it is known the electronic model can be understood, it is showed in the Figure 2.7.

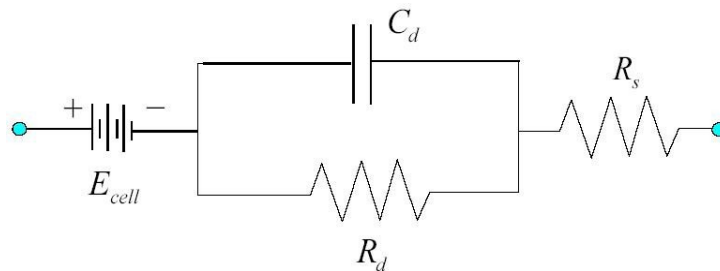


Figure 2.7. Electrode electrical model. Where E_{cell} is the half-cell potential, C_d and R_d the electrode impedance, and R_s the wires resistance.[1]

If it is analysed, one can realize the electrodes resistivity decreases with the frequency, also the *half-cell potential* effect decreases with frequency.

2.2.2 tetrapolar

At the beginning of the current section it is commented that the impedance measurement consists of applying a current and measure the voltage (or the opposite), and there are two methods to do it in a body by using electrodes, both are shown in the figure 2.8. First one uses the same electrodes to inject the current and measure the voltage, and in the second one, a different pair of electrodes pumps the current and measures the potential. First method is easier however it is not a good choice when electrodes are used, because the electrodes impedance is also added to the measure, which means that all the motion artefacts affecting the electrodes shall change the measure. A better option is the second well-called tetrapolar configuration [7].

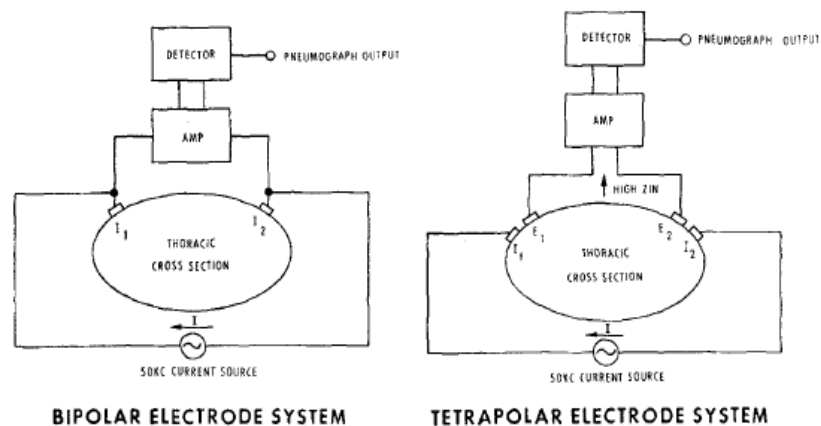


Figure 2.8. The two possible electrodes configurations for bioimpedance measurement. Left figure shows the bipolar configuration, the same pair of electrodes are used to inject and record the signal. Right draw is the tetrapolar schema, it use two pairs of electrodes, one to pump the current and the other to measure the voltage [7].

An ideal tetrapolar impedance measurement device should keep two conditions: (1) has the output impedance of the current source infinite and (2) the input impedance of the voltage sensing differential amplifier infinite. The first condition avoids the drop of current, keeping it constant even with load impedance changes. The second one gets the current that does not flow by the leads, hence the electrode impedance has not effect on the measured voltage.[2]

2.2.3 Electronic global model

The ideal conditions mentioned before are impossible to be obtained, a more realistic schema is proposed in the Figure 2.9. It includes a non-ideal current source with output impedance and stray capacitances, and a real instrumentation amplifier with common and differential input impedances, connected by electrodes to a body modelled by an impedance.

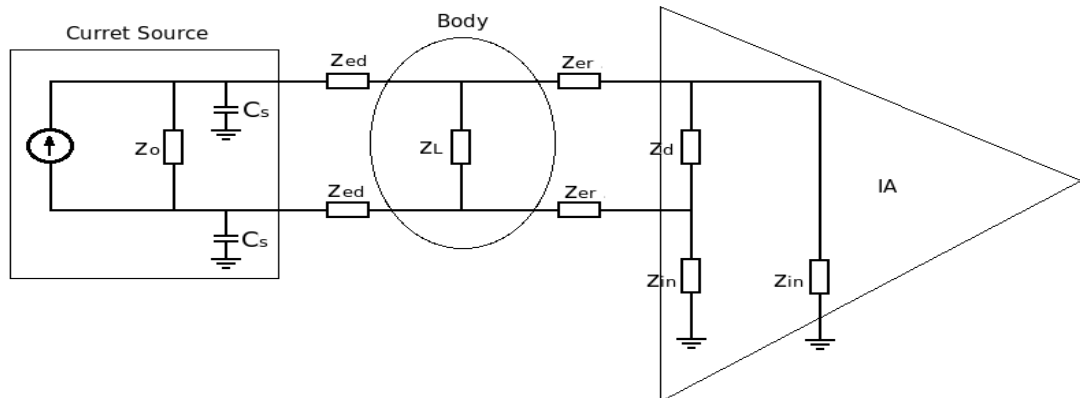


Figure 2.9. Non-ideal electronic model for a tetrapolar bioimpedance measurement system. Where Z_o is the output impedance and C_s the stray capacitance in the current source. The body is simplified as Z_L , connected to the device through the electrodes modelled as Z_{ed-r} . And the IA non-idealities differential impedance Z_d and input impedance Z_{in} . [8]

The independent behaviour of the main blocks are studied below.

2.2.4 Current Injector Properties

This section describes the usual problems in a bioimpedance current injector circuit. In order to understand these issues a simplification of the model chosen in the above paragraph is done.

The simplification is done having in mind just the current generated by the ideal source, the electrodes impedance is rejected because these do not have effects in the current, it leaves Z_d in parallel with the body impedance, where Z_d is very larger than the body impedance. This gives the Figure 2.10.

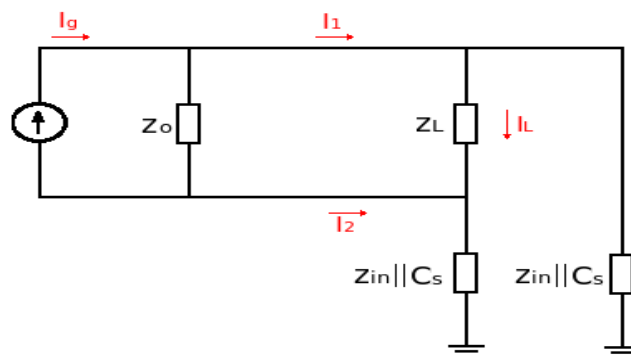


Figure 2.10. Global electronic model simplification in order to explain the current source problems.

Output impedance

To concentrate the interest in this issue $Z_{in}||C_s$ are supposed infinite in the Figure 2.10. With ideally infinite output impedance, the current generated is the same that the go back current, thus the current in the load impedance is well known.

$$I_L = I_1 = -I_2 = I_S \quad (2.1)$$

When the output impedance appears some of the current drops by there, then the current in the load impedance is unknown because it is correlated with the load impedance.

$$I_L = \frac{Z_o}{R_L + Z_o} \cdot I_G \quad (2.2)$$

However, the maxim error can be calculated knowing the highest load impedance value, where the error depends on the ADC resolution. Next formula shows the minimum output impedance to do not an error in the digitalization.

$$Z_o \geq (2^b - 1) Z_{Lmax} \quad (2.3)$$

For instance, in a system of 12 bits and supposing a maximum body impedance of 2k Ω , output impedance must be higher than 8M Ω [1].

A solution to reduce the output impedance is to place an inductor in parallel to resonate with the impedance, it may be made with a GIC (Generalize Impedance Converter), but this kind of circuit only works at one fix frequency and is rather complex. [9]

A better option is use a NIC (Negative Impedance Converter) circuit which emulates a negative value of impedance. Placing it in parallel creates an infinite impedance.[6]

Stray capacitance and Z_{in}

In the current source realization can appear some stray capacitances, these usually are quite small, but to work at high frequencies reduces the resistance (for example a 10pf capacitance at 500kHz is equivalent to 30k), then some of the current leaks to ground not only produced an useless consume but also a current reduction in the load. In addition if the quantity of leaked current is unknown load current as well.

$$I_1 \neq -I_2 \Rightarrow I_L ? \quad (2.3)$$

Same effect is produced by the input impedance of the IA, also some current can flow by there

Then only solutions for this are to improve the circuit, or to isolate the source and the IA to block the source current flow by the input impedance.[6]

Common mode voltage induced by the I_o offset

In a real current source the generated current is not the same that the absorbed. It produces an offset in the current signal, this DC component in the signal combined with the resistive part of the AI input impedance produces a CM voltage as huge as:

$$V_{cm} = R_{Zin} \cdot I_{off} \quad (2.4)$$

Even with a tiny current offset the huge Z_{in} produces a large CM signal. For instance an imbalance of 0,1% for a Z_{in} of 100M Ω /1pf generate a 50V.

The solution in this case is a large CMMR in the IA, or to isolate the current source to remove the current flow by the AI. (remember it is not acceptable to reduce the capacitance of Z_{in} in order to do not make the stray capacitance effect worse).[6]

2.2.5 Howland improved circuit

Usually the electronic circuits are commanded by a voltage supply, then to implement a current injector is necessary a voltage-to-current converter or also called transconductance amplifier, is a circuit able to provide a current output proportional to the voltage input. The main problem of this kind of circuits is to keep this proportionality when the resistive load changes, it is due to a real or virtual impedance in parallel with the load defines as output impedance. The current drops by this impedance thus the current in the output is not the expected, and because of this impedance is in parallel with the load, this dropping depends on the load in a non-linear way. Hence the ideal output impedance must be infinite.

The best circuit to get an infinite output impedance is the howland circuit.

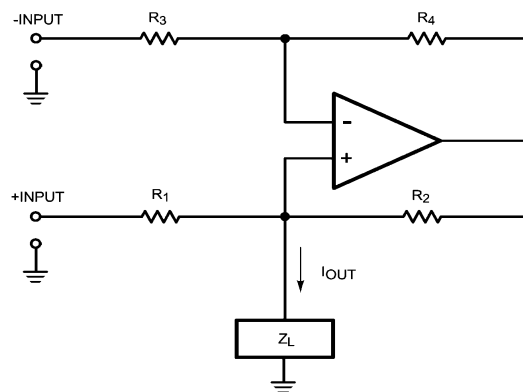


Figure 2.11. Electrical schema of the transconductance amplifier Howland circuit.[10]

It can be used to generate an inverted or non-inverted signal depending on which input the voltage change is applied [10]. One way to understand the circuit is seen it as a resistance in the positive input and a NIC in the negative, if this view is simplified by the Norton theorem is gotten a current source in parallel with a output resistance as the follow draw shows [11]:

$$R_o = \frac{R_2}{R_2/R_1 - R_4/R_3} \quad (2.5)$$

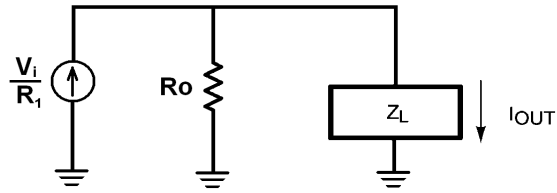


Figure 2.12. Electronic equivalent circuit after apply the Norton theorem.[10]

Where the the current is proportional to input by $1/R$ and the output resistance becomes infinite when this proportion is kept $\frac{R_1}{R_2} = \frac{R_3}{R_4}$.

However this circuit has a high waste of current dropping by R_1 , it could be solved doing a modification in R_2 yielding the “improved Howland” circuit [10].

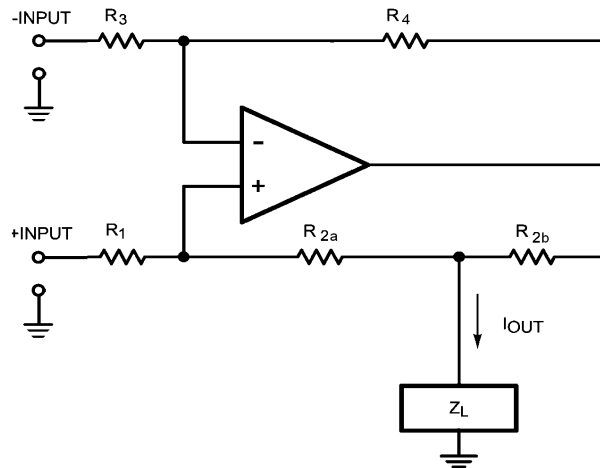


Figure 2.13. Electrical schema of the transconductance amplifier Improved Howland circuit.[10]

In this case the transconductance an the output resistance turn:

$$i_L = \frac{R_2/R_1}{R_{2b}} \cdot v_i \quad R_o = \frac{R_3 R_{2b} (R_1 + R_{2a})}{R_4 R_1 - R_3 (R_{2a} + R_{2b})} \quad (2.6) [12]$$

Theoretically if the resistances are matched to keep the proportion $\frac{R_1}{(R_{2a} + R_{2b})} = \frac{R_3}{R_4}$ the output resistance becomes infinite. But this circuit is especially sensitive to the resistance mismatches, even a 1% error resistance can be devastating to accuracy [13]. If the output resistance is calculated in the worst case the result is the follow.

$$R_o = \frac{R_{2b}}{2\varepsilon} \quad (2.7)$$

Where ε is the error in the resistance. For instances with a R_{2b} of $1\text{k}\Omega$ and 1% error, the output resistance could be only $50\text{k}\Omega$. Besides other factors influence in this output resistance working at high frequencies due to the OA non-idealities, these are the output capacitance because of the OA speed and the effects of the non-infinite open loop gain [13].

2.2.6 Instrumentation Amplifier

An instrumentation Amplifier is a type of differential amplifier with a group of special features, such as very low DC offset, very high CMRR or very high open-loop gain. The main function of it is the amplification of potential variations, like in this case the measurement of voltage linked with the bioimpedance changes.

However there is a usual problem which is of special importance when these amplifiers are used and specially important in bioelectronics, the common mode voltage. The target of the IA is amplify the voltage difference between the two inputs, but at the output this differential signal must have a reference ground, this ground may be connected to a power supply where is connected to the real ground. Moreover the body is connected by the air or by the shoes working as capacitors to the grid or other sources which have the same reference point. This generates a circuit as the showed it the figure 2.14, there, in addition with the differential source appears a common voltage, it is seen better in the simplification next to.

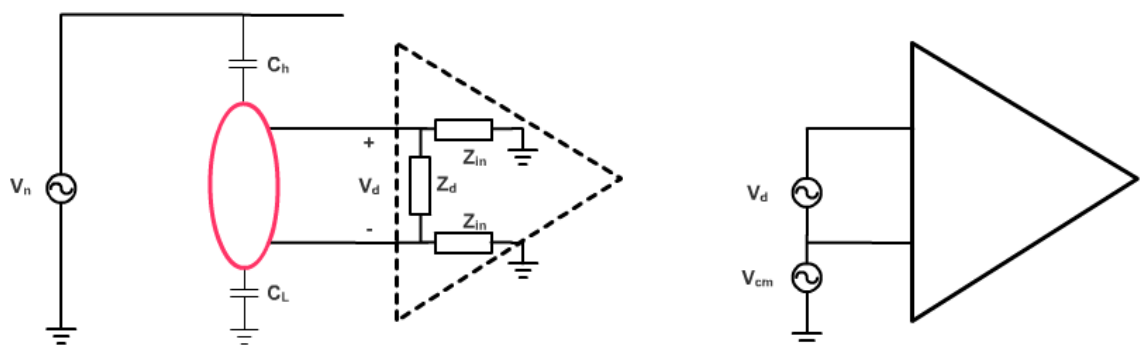


Figure 2.14. Explanation of the common mode voltage origin in the body measurement. Left draw shows a body (on pink) connected to an IA, with a noise source (usually the electrical grid) which is coupled by the capacitance between the wires or ground and the body. Due to the IA is also connected to the same ground appears a common voltage for both inputs, what can be simplified as the right schema.

This common voltage can not be rejected totally by the AI, and appears at the output as an offset, if this offset is high enough can degenerate in saturation. Furthermore in biosignal record it has a special disadvantage, a possible imbalance in the electrodes impedance because of artefacts, placement or composition changes the difference voltage increasing the common voltage.

The tendency of the device to reject the common voltage signal is called Common Mode Rejection Ratio (CMRR), a IA with a high CMRR is necessary to keep the well working of the acquisition. There are a lot of solutions to reduce this problem, and the best is to isolate the circuit, this way the common voltage disappears. [8]

2.3 Processing Background

2.3.1 Amplitude Modulation

The amplitude modulation is a technique used in communications for information transmission, it works by varying the strength of the transmitted signal in relation to the information being sent. It is achieved multiplying the original signal, or base signal, by a higher frequency sine wave called carrier signal, see figure 2.15.a.

If the same operation is seen in the frequency domain where the equivalent operator of the multiplication is the convolution, the result is a translation of the original signal power spectrum, until the carrier frequency, figure 2.11.b.

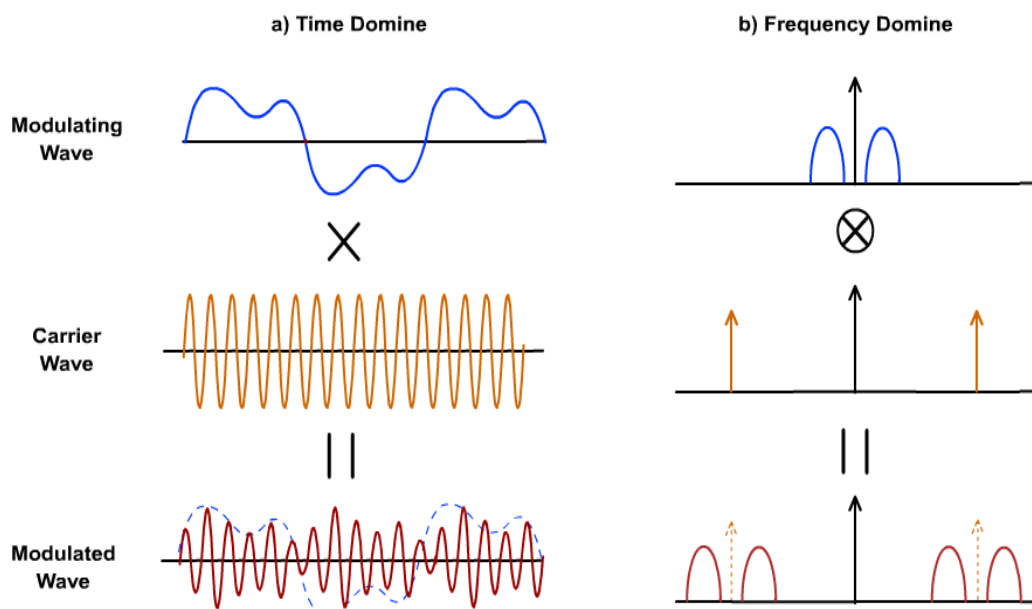


Figure 2.15. Amplitude Modulation explanation. a) shows the result of multiplied the carrier signal by the data signal in the time domain. b) Shows the equivalent process in the frequency domain.

To obtain the original signal an envelope detector is needed, which gets the amplitude variations in the carrier signal.

The main advantage of this technique is the chance to place the base signal power spectrum in a specific frequency range. It leaves to locate the signal in a low noisy spectrum area, and the simultaneous transmission of more than one signal at the same time, modulating the base signals by different carrier frequencies, setting these separated enough to prevent the aliasing between the neighbour bandpass signals. This frequency spectrum sharing method is known as frequency multiplexing. To get a specific base signal of the group is necessary a bandpass filter to reject the neighbour bandpass signals before the envelope detection.[14]

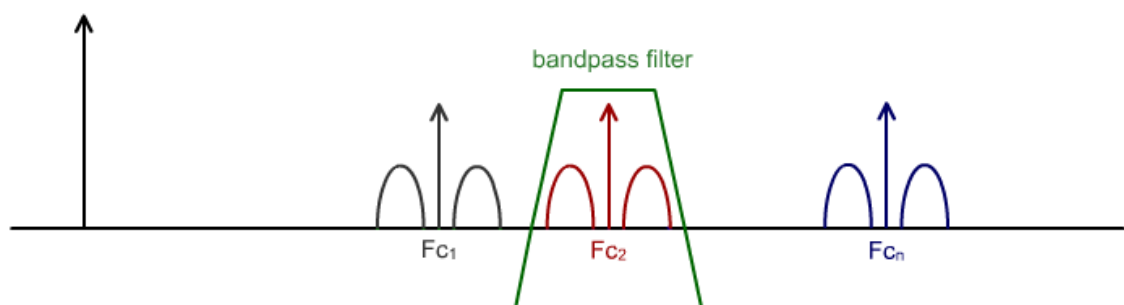


Figure 2.16. Multiplexing in the frequency domain. n signals transmitted at the same time using different carrier signals. A bandpass filter is used to get just the desired one.

2.4.2 Undersampling

Sampling is the process to digitalize a continuous signal, it consist of taking a equidistant samples of a continuous signal along the time. The minimum number of samples per second to provide a full representation of the original signal is defined by the “Nyquist–Shannon sampling theorem”. However, in special cases as in the AM, this rule can be broken, providing a sample frequency reduction which yields in the hardware side a decrement of the ADC work frequency required, it is especially important to work with high frequencies and more than one analog input. For instance, if the signal bandwidth is 100KHz and one ADC is shared to record 8 inputs the work frequency according with the Nyquist theorem (2.8) has to be at least 1,6MHz, the undersampling leaves reduce this frequency without loss information.

A simple way to understand the Nyquist theorem is to see the sampling as a multiplication of the original signal by a series of delta functions separated by the sample frequency. If this view is seen in the frequency domain, the furrier transform of the signal is a low-pass signal, the series of delta is a proportional series of delta, and the multiplication is the equivalent to the convolution, the result is a series of the original signal spectrum every sample frequency in the frequency spectrum. [14]

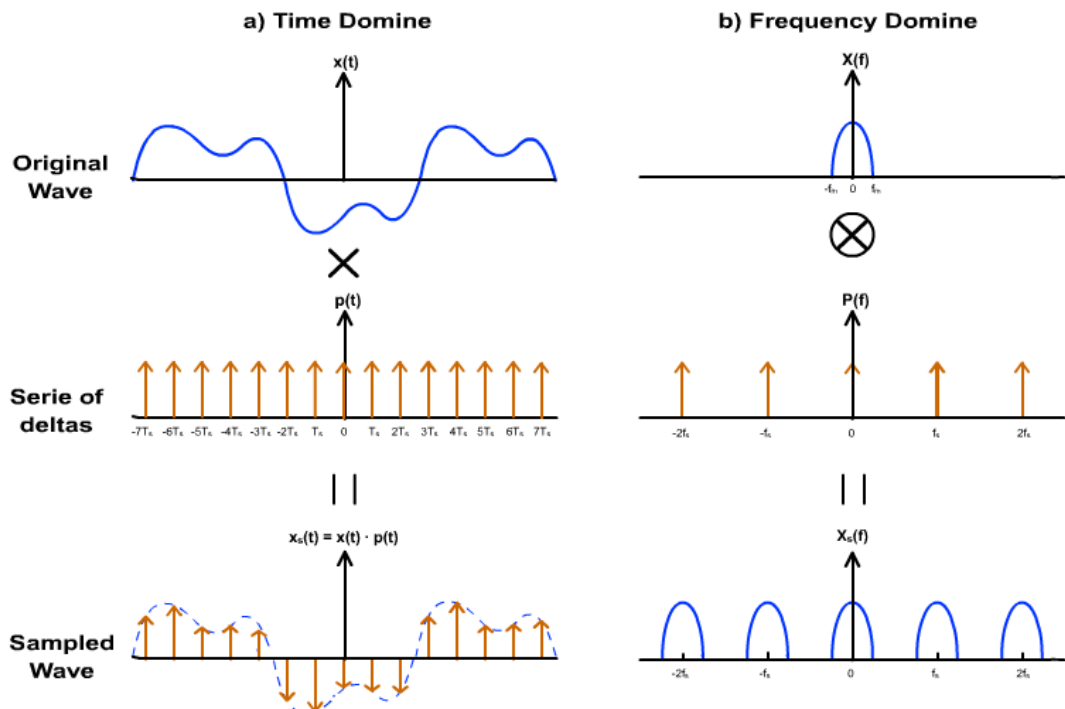


Figure 2.17. Normal sampling of a signal understand as the multiplication of the original signal by a delta series. Left figure shows the result in the time domain, and right one the equivalent in the frequency domain.

If the sample frequency decreases the aliases of the signal become closer, until one moment that the aliases overlap with the surrounding ones. This phenomenon is known as aliasing and causes a irreversible loss in the signal.

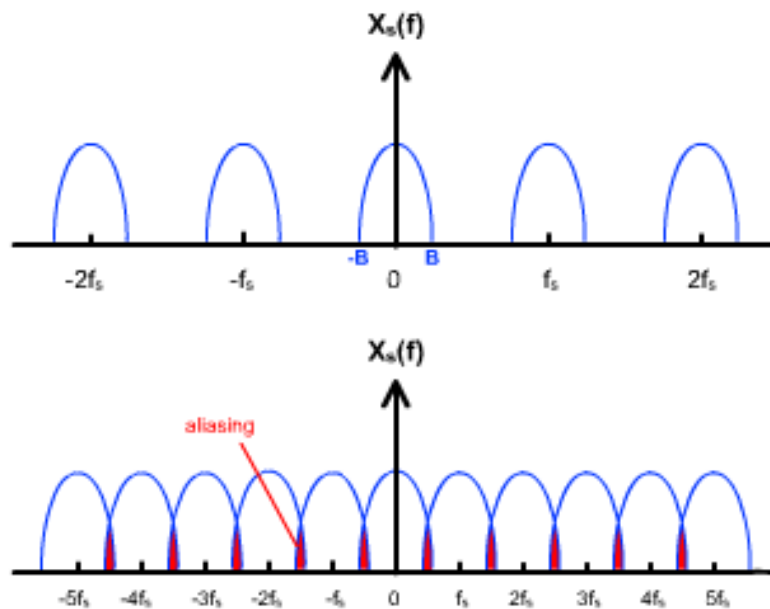


Figure 2.18. Aliasing phenomenon. The first chart shows the spectrum of a pass-band signal sampled at a right sample frequency (f_s). The second one represents the same for a smaller sample frequency, as small that it produces overlap with the neighbor aliases.

Hence the Nyquist theorem can be defined, the sample frequency must be bigger or equal to two times the biggest frequency in the low-pass signal.

$$F_s \geq 2 \cdot B \quad (2.8)$$

This theorem refers to the low-pass signal, however if the signal is passband (as in the AM signals) is possible to break the Nyquist theorem and to take samples at frequencies below the double of the maximum frequency without aliasing effects.[15]

The idea is simple, remembering that the sampling of a signal in the frequency domain means an infinite repetition of the sampled signal spectrum every sample frequency distance, and that a passband signal has a empty space between the two power spectrum lobes, thus is possible to calculate a sample frequency which places the aliases inside the original signal lobes, keeping the distance to prevent the aliasing.[15]

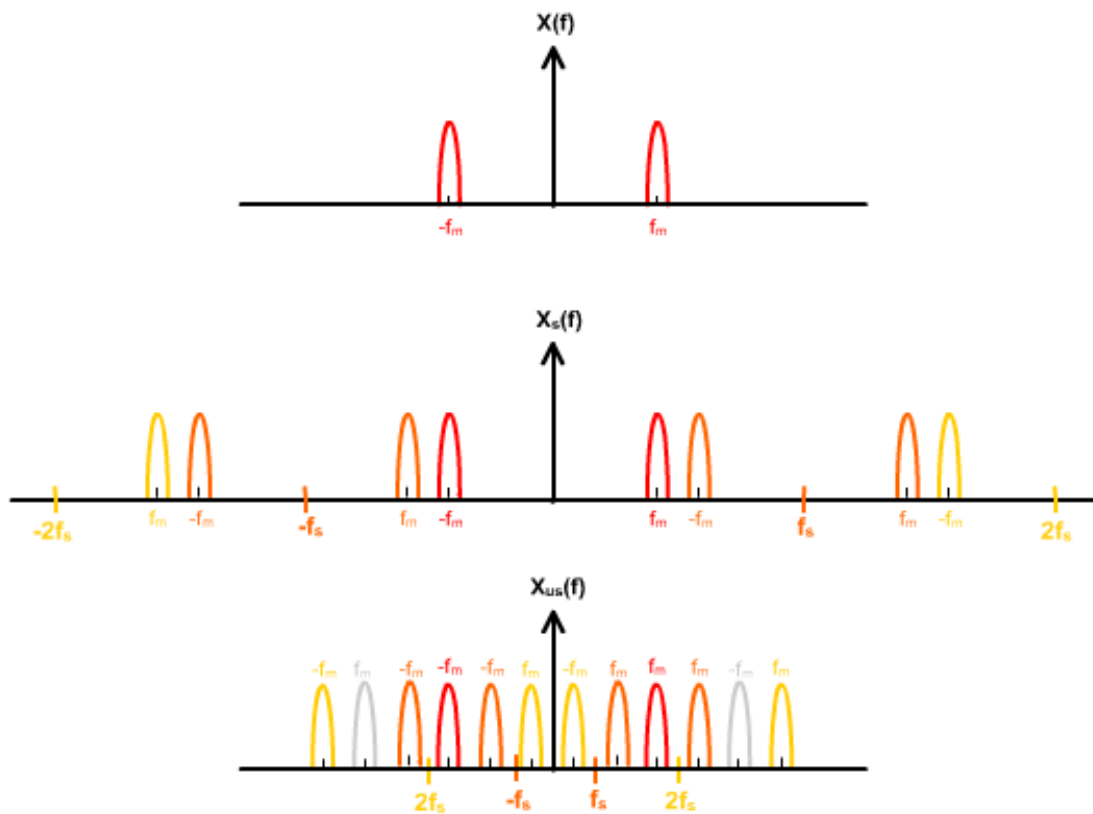


Figure 2.19. View of how a passband signal spectrum can be sampled below the Nyquist theorem without suffer aliasing. a) shows the passband signal spectrum b) passband signal sampled keeping the Nyquist theorem, the colors define the different aliases of the original signal, in this case remain a lot of empty space in the frequency band c) passband signal sampled at lower frequency that Nyquist theorem, the colors define the different aliases of the original signal, now the empty space in the original signal is used by the aliases.

The new condition for the sample frequency to prevent aliasing is:

$$\frac{2}{m} f_2 < f_s < \frac{2}{m-1} f_1 \quad (2.9)$$

Where m is an integer from 1 to f_2/B which represents the number of aliases between and the original band-pass. And $B = |f_2 - f_1|$.

However there is and other more visual way to understand the undersampling behaviour which is easier to manage, it is called 'fan-fold' paper method [16]. As it was shown above the sampled signal in the frequency domain is a repetition of the original spectrum every multiple of F_s , and the final interest area is just between 0 and $F_s/2$. An equivalent method to get the same view in this range consist of imaging that the frequency space is divided in blocs as the half sample frequency like in a 'fan-fold' paper. The resulting spectrum sampling at this frequency is equivalent to fold the stack of paper giving as result a superposition of the whole spectrum.

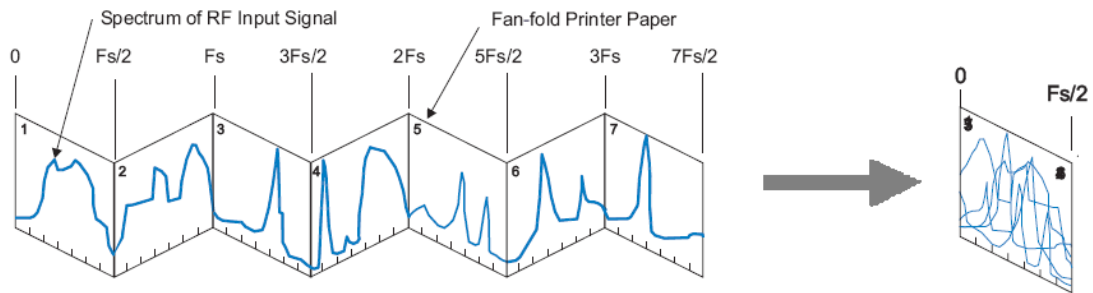


Figure 2.20. Fan-fold paper view. Left figure shows the spectrum of a random input signal divided in $F_s/2$ portions, and blended as in a fan-fold paper. Right figure shows the collapsed stack revealing the undersampled spectrum in the interest area 0 to $F_s/2$. [16]

Hence, if the original signal is an AM signal is highly recommended an antialiasing filter to prevent the higher or lower noise overlapping. Moreover by this method is easy to realize that the new frequencies of the collapsed spectrum can be calculated by the module of $F_s/2$.

$$F_{undersampled} = F_{original} \% \frac{F_s}{2} \quad (2.10)$$

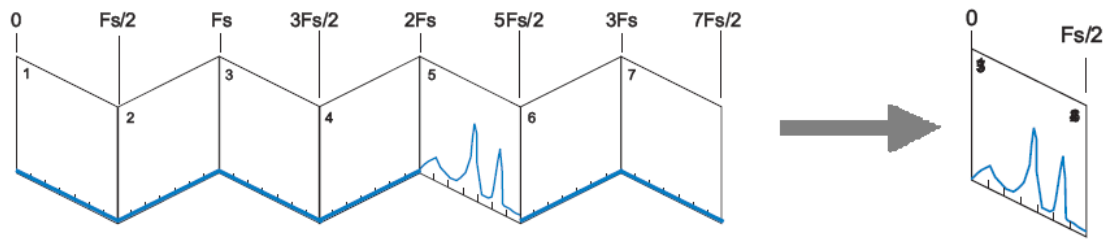


Figure 2.21. Fan-fold paper undersampling view for an AM signal. Left figure shows the spectrum of an AM signal in a fan-fold paper. Right figure shows the collapsed stack revealing the resulting spectrum and the new frequency of the signal [16].

3. Methods

The target of this thesis consists of finding out a method to record the bioimpedance in several points of a body simultaneously. In a first step a theoretical research is done, to seek the most adequate way to achieve the purpose, next the theoretical ideas are proved in a test device in order to confirm its correct working. Below all this is explained in detail in three sections, first tells the possibilities and reasons out the most suitable, second describes the building of test device, and third defines the testing process applied on it.

3.1. Multichannel Bioimpedance System Approach

This section speaks about the previous research in order to define the theoretical bases of the thesis. Stating from the aim all the possibilities to achieve it are analysed and compared, finally the best one will be chosen to implement the theories.

The final target is to build a system able to measure the impedance in several points on a same body at the same time and in an independent way. This thesis is a first research instead of a fixed device making, hence the features are not an imposition and the study has to develop depending on these. Anyhow, for a better future understanding, these are defined next together with the abbreviation is going to be used along the text:

- **Number of channels (N):** Number of bioimpedances that can be recorded at the same time.
- **Output Final Frequency (F_f):** Frequency the system provides a new sample in the output for every channel.
- **Injected signal Frequency (F_o):** Frequency of the current signal injected into the body is a sinus wave, it must be higher of 100KHz.
- **Body current limit:** the quantity of current going through the body is limited due to health issues to 1mA maximum.

As the background explains the best way to measure impedance is the current injection voltage recording tetrapolar configuration, it consist of injecting a current sinus wave by a pair of electrodes, and measuring the voltage changes using an other different pair of electrodes. Taking it as base, the target is to find out a system to use this method simultaneously in more that one place.

The obvious problem of the simultaneous measurement in a same body, is that the injected signals are going to affect each other. One way to analyze this, is seen the body as a shared element in a communication system, and the sinusoids as transmission signals going through this share channel. Under this view the share technique is the multiplexing, the two most basic forms of multiplexing are time and frequency multiplexing. These evolve in different ways to face up the problem, hence these have been group in to subsections.

3.1.1 Time multiplexing

General analysis

The temporal multiplexing can be implemented measuring each channel one by one and keeping the rest disconnected, but fast enough to seem these have been measured at the same time. It can be built using just a pair current source voltage recorder linked with the electrodes by an analog multiplexer which switch the signal to one group of electrodes.

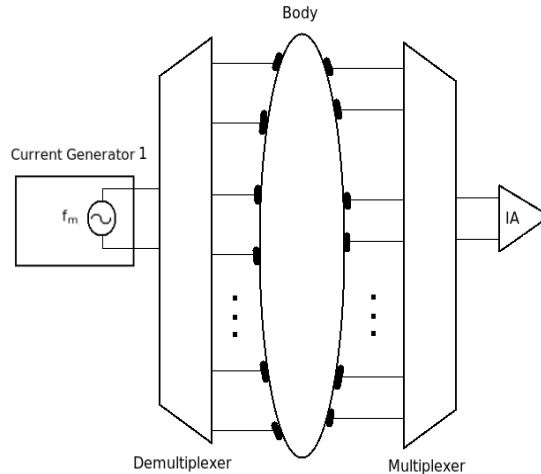


Figure 3.1. Time multiplexing first view schema. The current signal is injected and read in one channel at the same time using an analog multiplexer and demultiplex.

The output frequency of the system fixes the time period when the devices has to provide a sample of every channel. Using this schema the main signal is divided along the time to obtain a sample of every channel each output period. Hence the quantity of time an injected signal is used in a channel depends on the number of channels and the output final frequency, this share out is graphically showed in the next chart.

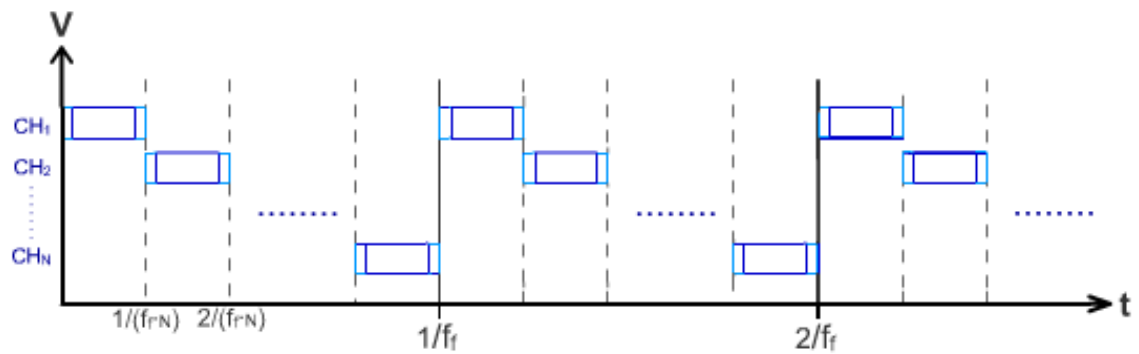


Figure 3.2. Distribution along the time of the recording lapses in each signal for a number of channels N and final out frequency F_f . The signals are divided in equal blocks for each channel every period of the final out frequency. Moreover is indicated on light blue the use of a small space of time between changes, for the system managing.

Then in order to get the amplitude and phase this pieces of information should be processed. The possibilities at this point depend on the requirements, however all these have a common limitation, the blocks of data are finites thus the set-up time must be reduced to do not waste the information. For instance if just the real part is wanted a simple envelope detector can be used, in this case the set-up time compromise with the ripple. If the imaginary part is required it may be needs a digital processing, this case the set-up can be an important limitation.

Electronic analysis

To examine the effects in the signal when the multiplexer are placed in both sides it is necessary to know the electronic model of these. The basic unit of a multiplexer is the analog switch, its model is shown below.

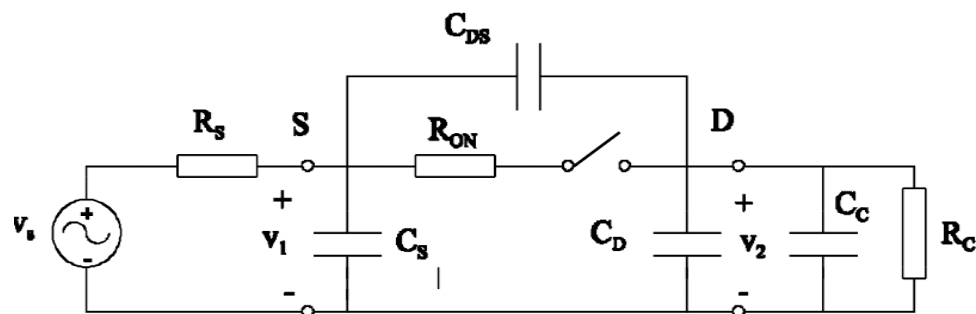


Figure 3.3. Electronic real model of the analog switch, the basic unit of the analog multiplexers. Where C_s is the capacitance in the input, C_d in the output, C_{ds} between the input and the output even when it id disconnected, and R_{on} the resistance of the device when it is driving a signal.

The value of the components in the best case found for the IC CD4053BC are $C_s = 5\text{pF}$ (on) 1pF (off), $C_d = 5\text{pF}$ (on) 3.5pF (off), $R_{on} = 120\ \Omega$.

A multiplexor or demultiplexer is a collection of switches where only one is switch-on. Thus the model of a multiplexer connected with electrodes to a body can be simplified as follow:

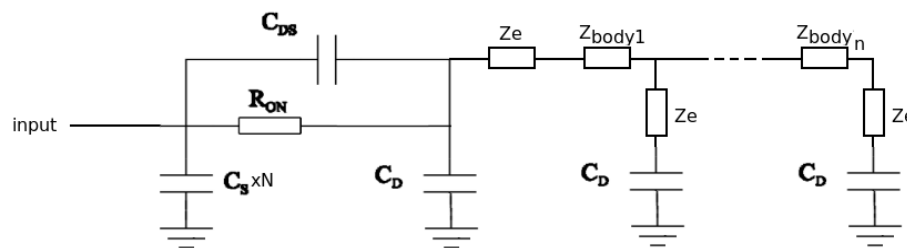


Figure 3.4. Simplified electrical model of a multiplexer connected to the body by electrodes. For the simplification the capacitance C_{DS} of the off switches has been rejected to be too big.

Analyzing the circuit is realized there are some paths to ground, to be precise four per every channel (because it requires a multiplexer for the current generator and its ground and for the IA and its reference). Due to all the inputs and outputs are connected to the body which have a low resistivity in comparison with the capacitors at 100KHz these can be seen as connected then appear a group of capacitances in parallel depending on the number of channels $C_{s_{on}} + C_{D_{on}} + N \cdot (C_{s_{off}} + C_{D_{off}})$. For instance, 10 channels and the IC found it yields 25pF which at 100KHz is about $60\text{k}\Omega$.

It can produce a leak of current, and the main point is that this leak can depend of the internal body movements or the artifacts.

3.1.2 Frequency multiplexing

General analysis

Frequency multiplexation consist of injecting signals of different frequencies for each channel simultaneously, to recording the sum of these visible in the voltage input, and taking the desired one filtering the group. However this view has an extra problem, even when the frequencies are different, if all the channels use the same reference ground the current which leaves a current injector is going to flow not only by its reference electrode but also by the reference electrodes of the other sources because all the grounds are the same. It produces an unknown distribution of the flow. The solution is to use independent sources for each channel, this way the current fed by the injection electrode flows back to the source only by its reference electrode.

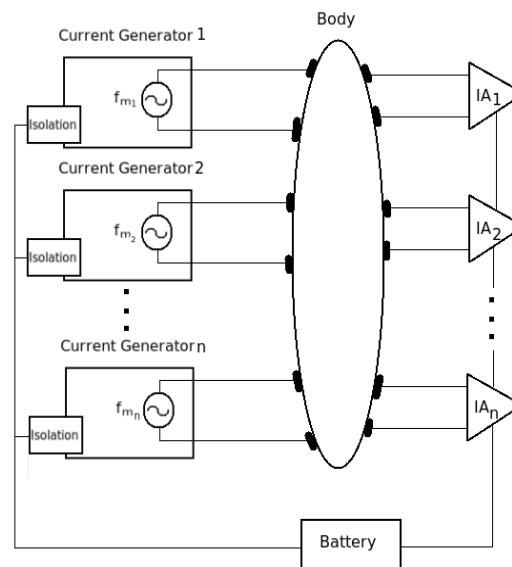


Figure 3.5. Time multiplexing first view schema. Every channel has an isolated current source. Because of the IA does not add any signal, these just read, can be fed with the same power supply.

Keeping the idea of seeing the body as a transmission share medium, this method is similar to the amplitude modulation (AM) communication system. Focusing in a single channel, the variations in the impedance changes the amplitude of the injected sine, as the base signal changes the amplitude on the carrier signal in AM.

Hence, increase the number of channels is equivalent to a multichannel AM system. Instead of modulating data signals by different carrier frequencies, the bioimpedance changes are modulated by the current injected waves. In this case the data signal of every channel is the bioimpedance signal between the electrodes, and the carrier the pumped sinus.

To prevent the overlap with the other modulated signals in the frequency domain, the carries frequencies must be established separated enough. In AM this share-out is obvious because the data signals are well known, however in this case the bioimpedance signal is the unknown factor. The trick is to follow the opposite deduction direction, the bioimpedance signal spectrum is unknown, but is known how precise the final recorded signal has to be, the final output frequency F_f , then to be sure the final signal is completely independent from the other signals in its ranges, it is considered that the impedance signal has and bandwidth as large as the F_f .

These ideas are explained in the figure 3.6, nevertheless it is just a schematic simplification, in a real body the bioimpedance variations depends each other or in case of be independents the current is flowing across whole the body “modulating” all the bioimpedance changes. Any way it approach guaranteed the impedance changes are not lost, because any change over the F_o in the impedance signal would not appear on the final signal due to has the same bandwidth.

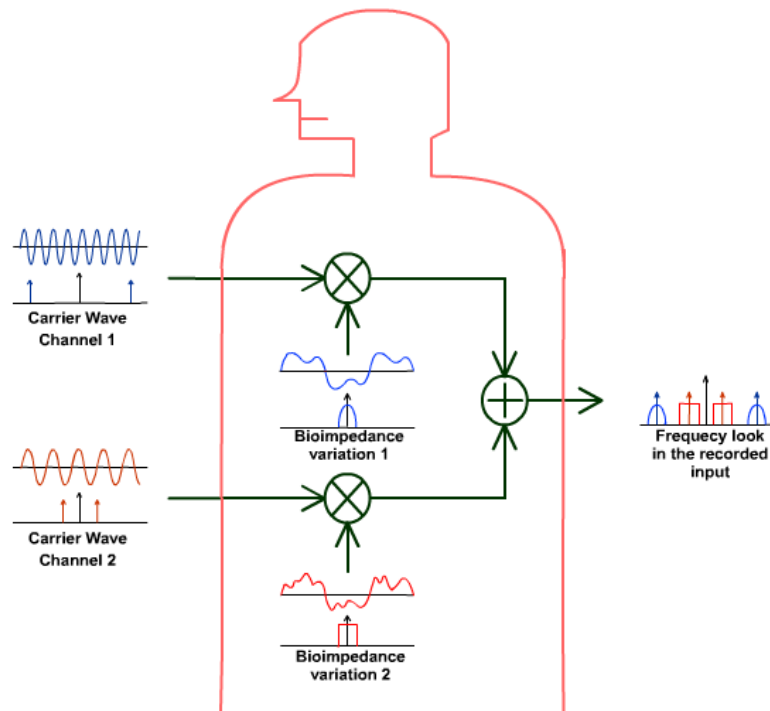


Figure 3.6. Comparison of multichannel frequency multiplexing with an AM transmission system. From left to right, two different sinus waves are injected in the body, these are equivalent to carrier signals in AM, inside the body the carriers change their amplitude depending on the bioimpedance variations as the data signals do it in AM. Owing to the carriers are flowing in the same medium these are added, the result when the potential variation is recorded is a distribution of the bioimpedance signal spectrums in the frequency domain.

Then in every voltage record point the extracted signal contains a sum of all the injected and body-modulated waves. As in AM to obtain the wanted one, a filter is needed. There are a few ways to share the frequency spectrum the best option thinking in the filtering is place the carrier frequencies as far as possible to increase the rejection, however it can be better to have close frequencies carriers to do all the circuits equals simplifying design. In any case the realization of the filter can be analog or digital, the analog one always has more non-idealities and implementation problems, and the digital requires the digitalization of the signal. For the digitalization of signals about 100KHz according with the Nyquist theorem the sample frequency must be above 200KHz, nevertheless in this case the undersampling technique can be used.

The undersampling is really a good choice for this schema, the carrier frequencies can be kept as close as possible, then this group of lobes can be seen as a only base signal translated in the frequency by a modulation, where this group can be replaced in the low side of the spectrum by using the undersampling. It is easier to understand looking at the figure 3.7.

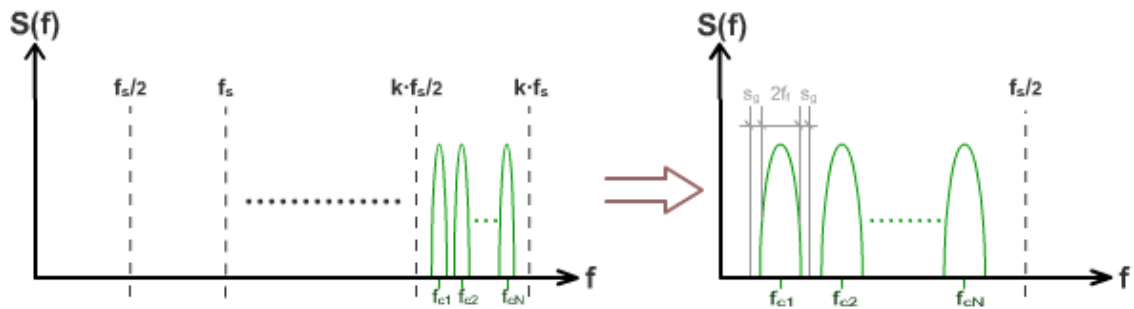


Figure 3.7. Effect of undersampling applied to a group of modulated signals. The left image shows the distribution of N signals with bandwidth the final output frequency F_f modulated by different carriers in the positive side of the frequency spectrum. The right figure is the result in the frequency domain of the left spectrum after applied undersampling at the sample frequency F_s . The right image also shows the most efficient distribution of the signals depending on the basic constants, N and F_f , and in this case a new variable F_s , placing the cluster in the middle and leaving a safety gap S_g in between.

Like in the previous section, the share-out of the signals can be expressed, this occasion in the frequency domain, depending on the number of channel N and the final output frequency F_f . F_f fix the bandwidth of every modulated signal, and N the number of these, for a right use of the frequency space all are put together leaving a security gap S_g in between. Then the group looks like a single signal with bandwidth:

$$BW = N \cdot 2(F_f + S_g) \quad (3.1)$$

Hence the carrier signals F_{cN} and the sample frequency F_s can be combined to locate this cluster in a good position for a correct undersampling.

Electronic analysis

The first step is to analyze the one channel behaviour, taking the electrical model of the *figure2.9*, and simplifying it considering just the current flow of the independent source, the circuit is shown below:

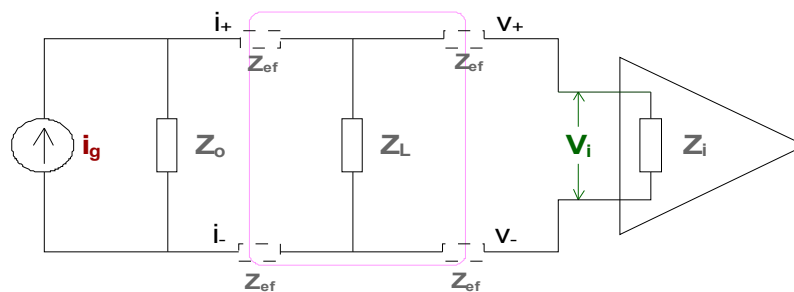


Figure 3.8. One independent current channel restive load simplified view when it is connected to a body together with the IA. Where Z_o is the current source output impedance, Z_L the load impedance, Z_i the IA input impedance and Z_{ef} the equivalent impedance of the electrodes and the flesh till Z_L . V_i is the voltage seen by the IA.

Usually the electrodes pair V-I are placed as close as possible each other, and the electrodes impedance is minimum, thus the Z_{ef} could be rejected. Then the impedance measured is a parallel combination of the three remaining, hence the error in the load impedance is non-linear and change with its value.

$$\epsilon = Z_L - \frac{Z_L \cdot Z_{eq}}{Z_L + Z_{eq}} = \frac{Z_L^2}{Z_L + Z_{eq}} \quad (3.2)$$

$$Z_{eq} = Z_i || \pm Z_o$$

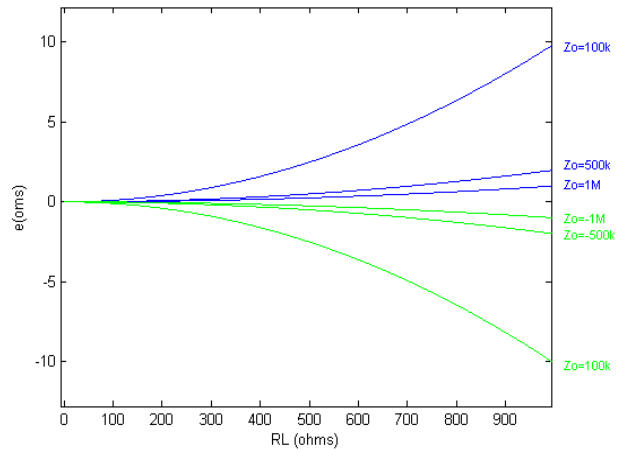


Figure 3.9. Representation of the error changes depending on the load impedance Z_L in the range $[0,1K]\Omega$ for different values of Z_{eq} . Where Z_{eq} is the equivalent impedance of all the impedances in parallel with Z_L in this case, the instrumentation input impedance, and the current source output impedance.

Obviously to reduce this error the Z_{eq} must become infinite and this is usually quite high, but is going to be showed below how the addition of more channels reduces it quickly.

And other way to skip this error without changing the circuit is estimate the Z_{eq} , it could be done using autocalibration techniques [17]. However it is explained later why it is also inappropriate when more channels are added.

When more channels are connected to the body the schema of the figure 3.8 becomes on the following one:

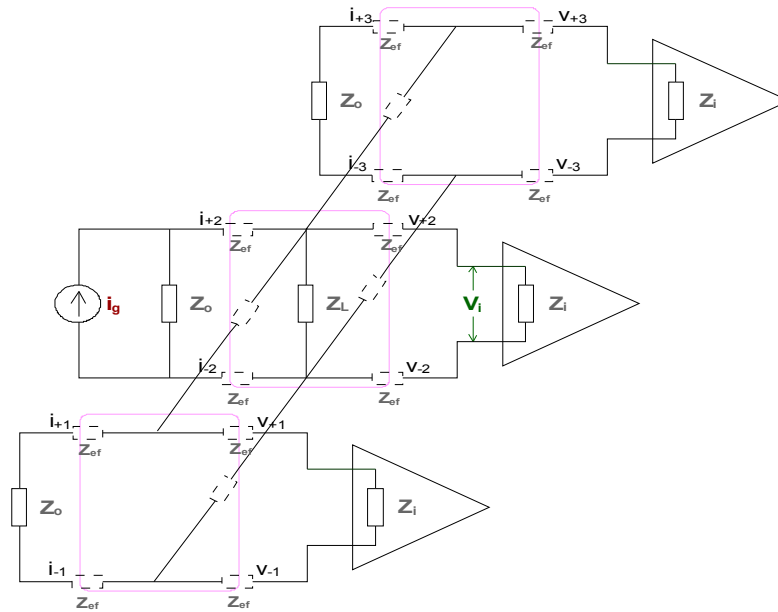


Figure 3.10. Electrical schema of the resistive load for one current source when N channels are connected to a body.

In this case and keeping the above vision, for every channel appears an output and an input impedance which are connected in parallel with the under measure channel through the body impedance between the electrodes of the different channels. These impedances in between depends on the distance from one channel placement to the other, but usually even if it is placed in far points the resistance should be smaller than the output and input impedances, thus it could be rejected. It yields an error, considering the worst case where all the output impedances have the same sign and value.

$$\epsilon = Z_L - \frac{Z_L \cdot Z_{eq}}{Z_L + Z_{eq}} = \frac{Z_L^2}{Z_L + \frac{Z_{eq}}{N}} \quad \text{where } Z_{eq} = Z_i || \pm Z_o \quad (3.3)$$

Every channel connected adds a Z_{eq} in parallel to the load decreasing the total value and increasing the error in a proportional way.

As it was discussed previously, one option is the autocalibration, nevertheless this choice involves calculating the calibration of each combination of channels and select which channels are connected if not all the channels are always used at the time. In addition with this method, the internal body resistive connection changes should not affect to the measure due to the tiny variation, however the artefacts produce higher variations which would influence in the neighbour channels.

Hence the best option is provide a Z_{eq} large enough not to affect the load bioimpedance, keeping in mind the number of channels.

3.1.3 Conclusions

Both methods have their own problems and their own improvements. Next the decision of take one instead of the other is discussed.

As it has been mentioned along this text, this thesis is viewed more as a research than a fix aim project, then even when in a first analysis both seem feasible and probably the time multiplexing option is easier to develop, the frequency multiplexing is chosen.

The main reasons are the flexibility and scalability, the time multiplexing is a more rigid schema, if the number of channel is increased it is as well needed to change the hardware and the quantity of samples is reduced. It can be understood by checking the figure 3.2, the increase of the final frequency F_f or the number of channels N involves a reduction in the blocks of data, it means a loss in the precision because the window to average a sample every F_f decrease. Whereas for the frequency multiplexing (figure 3.7) a rise in N or F_f yields a growth in the spectrum that can be adjusted increasing a bit F_s and recalculating the carrier frequencies, owing to the sample of every channel remain at equal lapses there is not loss in the precision. Moreover the addition of N does not need changes the hardware, it just requires to add an independent pair current source voltage recorder.

Like it has been sketched above other advantage of the frequency multiplexing is that the look to the signal is not confined in a small lapse every F_f , in this case the signal is recorded along all the time and the channels rejection is made in the frequency level. It provides an extra possibility, the effects of all the other current injected signals into the body can also be measured from any voltage recorder without any change in the software.

Finally, a last important cause related with the research approach of the thesis, is the opportunity to test this idea not developed yet, specifically the AM treatment and the undersampling. Because of this novelty it can bring some new ideas of application, specially the property of the simultaneous measurement of the other pump signals from every channel.

3.2. Prototype Device

After having chosen the option, it is continued with the implementation of a prototype device where the theoretical approach is proved. First of all, an introduction of the global schema is defined, the concrete details of some parts are grouped in subsections.

The first step is to define the basic constants of the system, the idea is to test the possibility of building an eight channels device $N=8$, with and final output frequency of $F_f=200Hz$. All the calculations will follow these bases however instead of making all the hardware, just three channels are going to be made in order to measure the effect of the more close neighbour signals, in the frequency domain. Then the device will be able to configure the carrier frequencies of the three channels to test the results of eight possible channels. In addition to reduce the complexity the devices is going to measure

only the real part of the impedances, it means the amplitude of the signal, thus the phase changes in the circuit are forgotten.

As above is explained, to obtain the independence between the current signals, these should be fed by independent sources. The best option would be isolate the sinus signal, but the actual analogical isolators do not work at 100KHz. Hence the suggested configuration is to isolate the signal generator and the current injector, the signal generator proposed is a DSP which is managed digitally, thus the digital control signals and clock also have to be isolated.

To separate the independent circuits isolated DC-DC sources could be used. This kind of sources transforms the electrical energy in electromagnetic energy which is transmitted by a good magnetic material and converted again in electricity. According with the electromagnetism laws this energy conversion only is possible with alternating electricity, thus the DC power input must be converted to AC to be transmitted as electromagnetic energy and changes back to DC. This system produces problems as an irregular consume in the current due to the AC conversion, and an electromagnetic coupled noise, hence additional methods should be used to keep a low noisy supply, because voltage stability affects in the precision.

The voltage acquisition side may be conditioned by a IA which prepare the signal to be digitalized in a ADC, between these an antialiasing filter is highly recommended in order to reduce the undersampling issues. All the IAs can be fed with the same non isolate supply.

Summarizing, every channel has an independent current injection source made up of a (1) DC-DC isolator to feed the independent circuit, (2) a voltage regulator to keep a stable supply, (3) a DSP to generate the sinus wave, (4) a digital isolator to communicate the main circuit with the isolated DSP, (5) the voltage-current converter to inject the current by the electrodes, and finally outside of the isolated circuit an (6) IA connected to a (7) ADC through an (8) antialiasing filter.

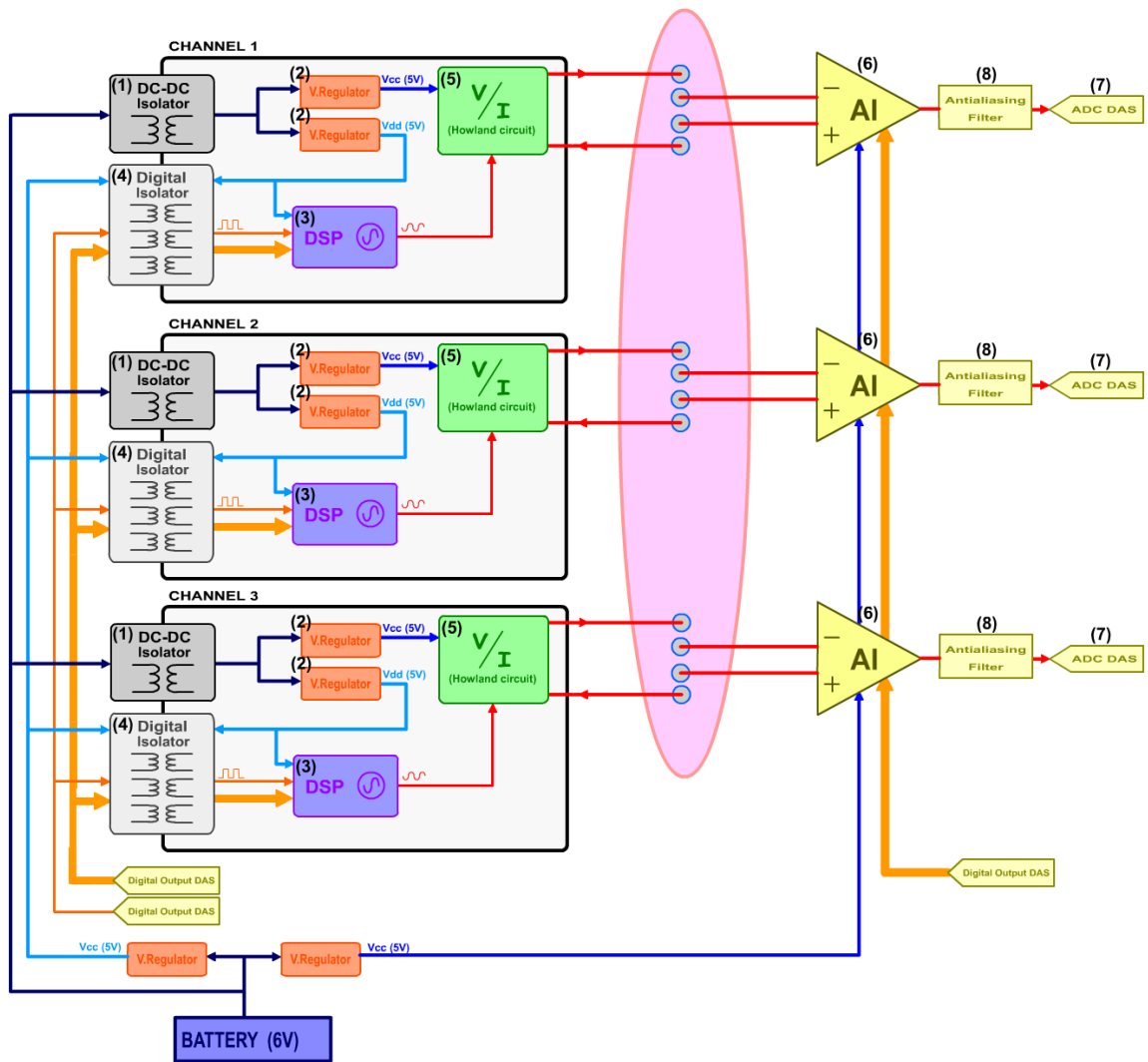


Figure 3.11. Test board global schema. The power connections appear on different blues, deeper blue for the main supply, blue for the analog supply, and light blue for the digital supply. Connections on red are analog signal, and on orange the digital signals.

3.2.1 Voltage to Current Converter

In the chosen configuration a constant current signal is injected into the body and the voltage variations are measured. It means the sinus wave from the DSP must be converted to a current signal, it is done by using a voltage-current converter.

It is a special block because does not exist as a pre-build circuit, it is custom-made, thus the properties depend on the circuit, the components and the frequency. Hence it should be studied and customised to obtain the right properties, the features for the present system are discussed now:

1. **Transconductance:** the relationship between control voltage and output current may be linear in the whole range, and the value depends on the number of channels. The current flowing into the body is limited for healthy issues and for the AI input

range (if the maximum impedance expected for the body is 1k the current going through it must produce a voltage less than the AI's input range, in this case 5V) to 1mA. Moreover the total current in the impedance is the sum of all the currents flowing by it, thus in the worst case all the injected currents would go into the load impedance therefore the total would be the sum of all. For these reasons the injected current for each channel must be:

$$I_{Omax} = \frac{1 \text{ mA}}{N} \quad (3.4)$$

The input wave comes from the DSP with a value of 612mVpp, then the transconductance will be about:

$$\frac{I}{V} = \frac{1.6}{N} \text{ mA/V} \quad (3.5)$$

In this test case with N=3 it is 0.54 mA/V

2. **Output Impedance:** it has to be high enough in order not to affect the linearity, it depends on the ADC resolution, as is explained in the formula (2.3). In a case with more than one channel this formula should be multiplied by the number of channels because of the other output impedance in parallel divide the value as has been seen in the section 3.1.2.

$$Z_o \geq (2^b - 1) Z_{Lmax} \cdot N \quad (3.6)$$

Then for a resolution of 12 bits, a maximum body impedance of 2kΩ, and three channels, the output impedance must be higher than 24MΩ.

3. **Output offset and stray capacitances:** tiny imbalances between the injected and return current produces a current offset which flows by the AI, raising the CM voltage (see section 2.2.4), however in this case the current sources are independents, thus pumped and return current are the same. In this case this parameters are not critical.

For the circuit an “improved Howland” has been chosen. It is a one op-amp circuit with low output impedance and low leaks of current. To get the desired high output impedance a trimmer is placed in series with R3.

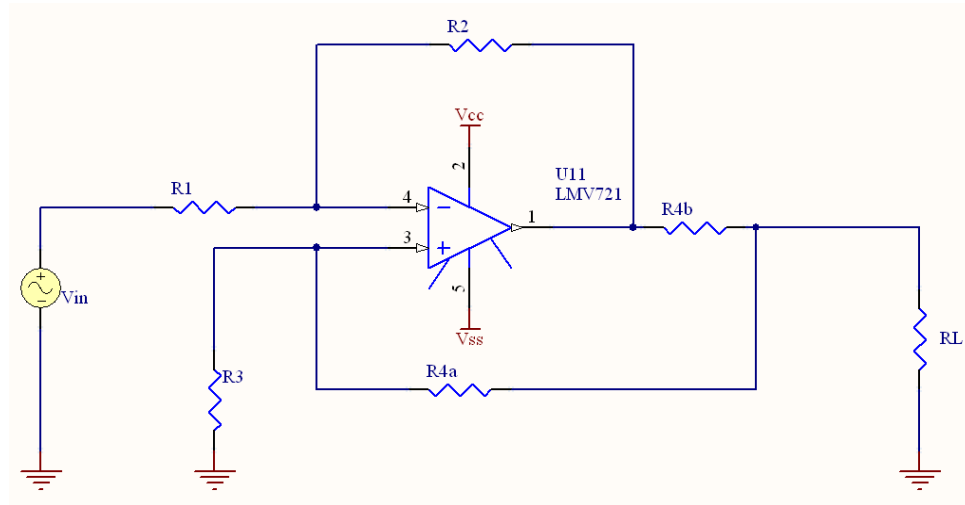


Figure 3.12. Modified Howland in the non-inverter configuration, used as voltage to current converter.

The formulas to calculate this circuit are:

- Transconductance:

$$\frac{I_o}{V_o} = \frac{R_2}{R_1} \cdot \frac{1}{R_{4b}} ; \frac{R_2}{R_1} = \frac{R_{4b} + R_{4a}}{R_3} \quad (3.7)$$

- To avoid the saturation in the load.

$$|V_{Lmax}| < (V_{sat} - R_{4b} \cdot |I_o|) \quad (3.8)$$

Where V_{Lmax} is the maximum voltage in the load in this case

$$|V_{Lmax}| = I_{Omax} \cdot R_{Lmax} = \frac{I_{BODYmax}}{N} \cdot R_{BODYmax} = \frac{1 \text{ mA}}{N} \cdot 2 \text{ k} \Omega \quad (3.9)$$

for thee channels 0.66V and V_{sat} the saturation voltage of the op-amp (2.5V).

- To reduce the current leak: If $R_{4a} \gg R_{4b}$, then the current that flows to ground by R_{4a} decrease.

The op-amp chosen has to keep at least the next conditions, to be rail-to-rail, to have low output offset and low noise, and to work and be stable at the work-range frequency (100 – 110 kHz) and load resistance range (100Ω – 2kΩ), and to have a bias current lower than 10nA [45]. After some tests one who satisfies this is the LMV721 [18].

3.2.2 Instrumentation Amplifiers

As IA a commercial one has been chosen, the model is AD8221. It has the nowadays highest CMRR, and the gain is controlled by a resistor.

The inputs must be grounded to provide the current a flowing path, it is made by placing a 1M resistor, furthermore it is used to make a 50Hz rejection filter adding a capacitor to improve the CMRR.

This input seen from the current injector, which is independent of the current path ground, appears as a two series resistors in parallel with the differential input impedance of $100G||2pF$ [19].

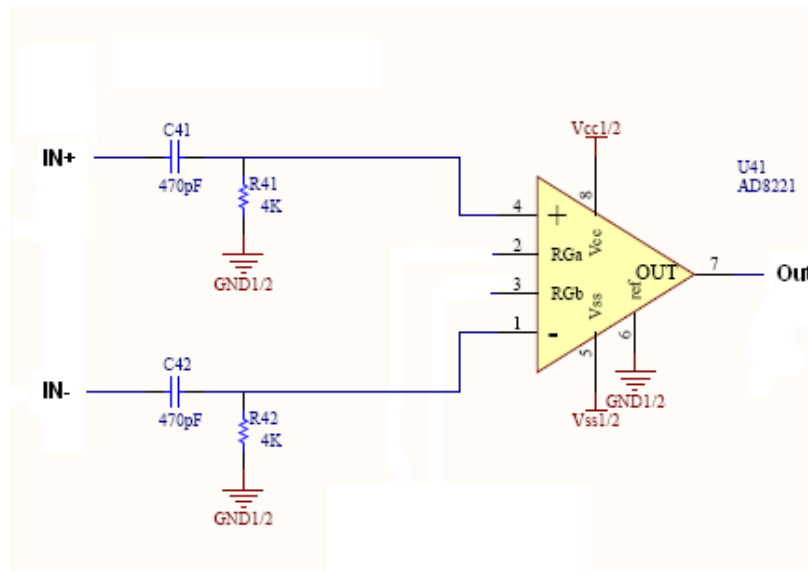


Figure 3.14. Instrumentation Amplifier electronic model. It shows the bias path used as low pas filter.

If this configuration is calculated the equivalent input impedance at 100KHz has a value about 570K.

To control the gain a digital potentiometer is connected to the IA. The model is AD5165, and the main features are 8 bits and 100K 20%. This 20% of margin error made the result rather imprecise, it forces to do a digital correction once the signal has been acquired [20].

3.2.3 Antialiasing filter

When the undersampling technique is used the addition of an antialiasing filter is extremely important. Like the background explains, the undersampling produces an overlapping in the frequency domain, thus all the possible signals such as the noise of the circuit or biopotentials can affect the modulations, a band-pass filter for the work range rejects the signals which could overlap with the wanted ones. For this aim a one Op-Amp filter is added, and it is used also to duplicate the IA output which had an output swing of [1,1 to 3.8]V.

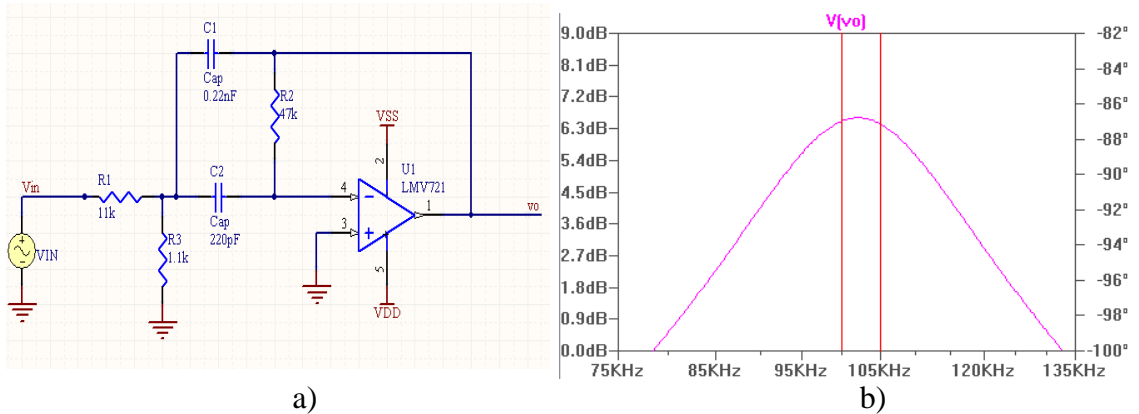


Figure 3.15. a) Multiple feedback band-pass filter electrical schema. b) detail of the frequency response, the red vertical lines delimit the working area [100,105]kHz.

It is a simple first grade filter, and the work band is quite spread, thus as the figure3.15. shows the gain is not equal for the different frequencies, for a higher precision system it can be calibrated by software.

3.2.4 Processing

Here not only the treatment of the data is explained but also the decision to fix the carrier frequencies and the sample frequency, because it is going to affect the rest of the process.

With the global features established for the test device, the calculation of the carrier frequencies and sample frequency can be done following the ideas of the section 3.1.2. The final output frequency is $F_f=200Hz$, and the number of channels $N=8$, thus theses can be placed leaving a security gap of $50Hz$, according with the formula (3.1) the total bandwidth is $4KHz$. The easiest way to apply the undersampling is to take a F_s of $10KHz$, hence the frequency spectrum appears divided in $5KHz$ regions, these will collapse to provide the undersampled spectrum according with the “fan-fold paper” view (section 2.4.2). Then the $4KHz$ BW cluster is placed in the middle of the $100KHz$ sector, it yields eight carrier frequencies from $100750Hz$ to $104250Hz$ separated by $500Hz$. These frequencies become to new ones from $750Hz$ to $4250Hz$ (still separated $500Hz$) after the undersampling.

Table 3.1. Define the frequency of the injected current signal for every of the eight frequency channels, and the resulting frequency after the undersampling at $f_s=10000Hz$.

Channel	f_1	f_2	f_3	f_4	f_5	f_6	f_7	f_8
Output Frequency	100750Hz	101250Hz	101750Hz	102250Hz	102750Hz	103250Hz	103725Hz	104250Hz
Undersampled frequency	750Hz	1250Hz	1750Hz	2250Hz	2750Hz	3250Hz	3750Hz	4250Hz

In the digital side the first step is to apply a filter to the input to get the desired signal from the group, it is done by using a band-pass IIR filter. This kind of filter has been selected due to it gives a better filtering with lower filter orders, however it has a poor response for the phase, this feature is not important in this case, but should be kept in mind for a whole impedance measurement. The parameters of the filter are a central frequency equal to the chosen carrier frequency with a bandwidth as broad as the bioimpedance signal BW plus the security lateral gaps.

$$f_o = f_c$$

$$WB = 2 \cdot (f_f + Sg) = 2 \cdot (200\text{Hz} + 50\text{Hz}) = 500\text{Hz}$$

The filter provides a sinus wave with variable amplitude, the bioimpedance signal is coded in this amplitude, thus to get this amplitude changes a software envelope detector is implemented. The classic way to get it is by the absolute value of the Hilbert transform [21]:

$$S_{envelop}(k) = |H\{S_{filter}(k)\}| \quad (3.10)$$

This method is good enough, but the Hilbert transform is a window method, it has to be applied to a block of samples, and the result is inexact in the extremes because of the shortage of samples around. The proposal is to implement a sliding window algorithm with a extended window, it means a window which also takes both sides neighbors samples to operate the Hilbert transform but removes this from the final result. The size window chosen is the final output period $1/f_f$, with a safety extensions of the same value, its size in number of samples is $f/f_f = 50$, after to obtain a single value every output period the average of the window is calculated. It is graphically explained in the figure 3.16.

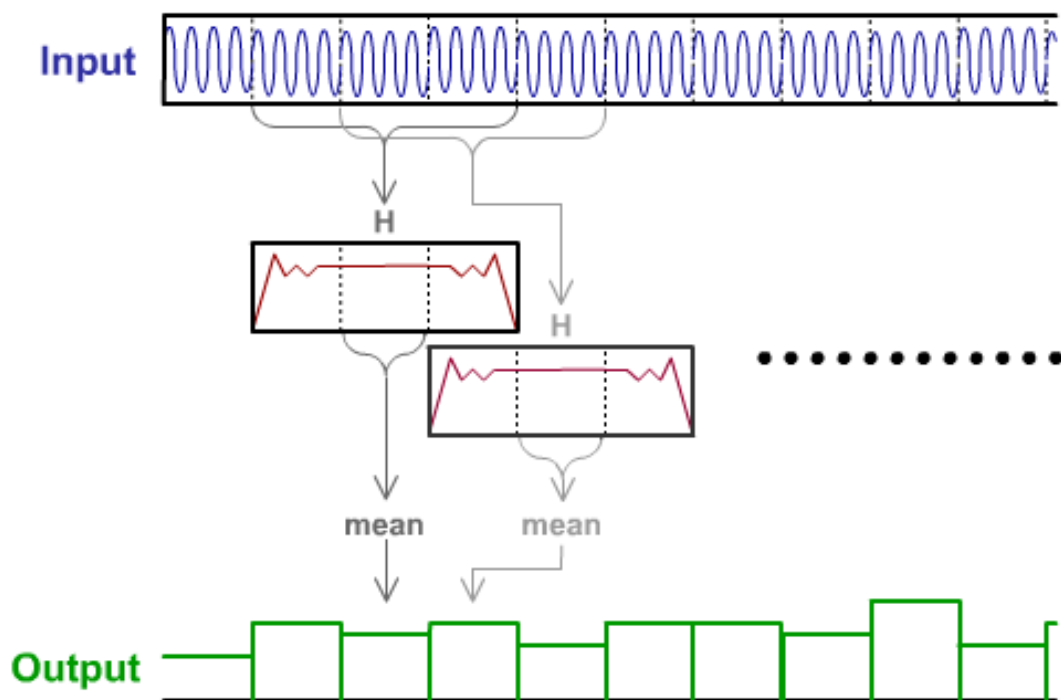


Figure 3.16. Sliding window algorithm to get the sinus wave envelope by the Hilbert transform. The algorithm takes three blocks of 50 samples from the input signal, calculates the Hilbert transform and takes the 50 middle samples to calculate the mean and provide a final sample for the output. Next the window moves 50 samples in the original signal, and repeats the process.

The features chosen produce suitable results and quite similar for all the frequencies (see test and results sections x.x and y.y). The inconvenient is the operational resources consumption, the Hilbert transform uses the Fourier one, rather slow even using the FFT, this aspect should have a deeper study looking for the best compromise speed versus SNR. Some ideas can be changing the size of the window in this schema, applying other techniques well-know in the AM area, or dedicate algorithms [22].

Finally the block diagram of the processing side is shown below.

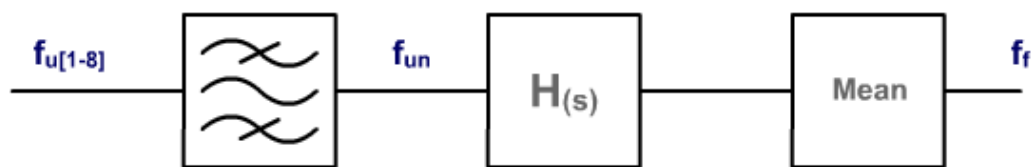


Figure 3.17. Blocks schema of the processing, it consist on a bandpass filter to chose the channel signal, the envelope detection by the Hilbert transform, and the average of the signal to adjust to the final frequency.

3.3. Calibration

The margin errors and non-idealities of the components in the circuit, makes the result slightly different from theoretical value, most of the case this variation is systematic and can be guessed by using a standard reference, it is known as calibration. This section describe three different adjusts which must be done in the same order, because one support the others.

3.3.1 Current source output impedance calibration

As was discussed previously the output impedance causes a non-linearity in the measure, and the best way to reject it is trimming the circuit (see section 3.1.2). However the error ranges make this task more complicated than it could seem. Following a deep understanding is discussed to find the more appropriated method to get it.

A first condition is to study the error behaviour. With infinite output impedance the load current would be equal for any load resistance, but when it is a finite value load current acts as following:

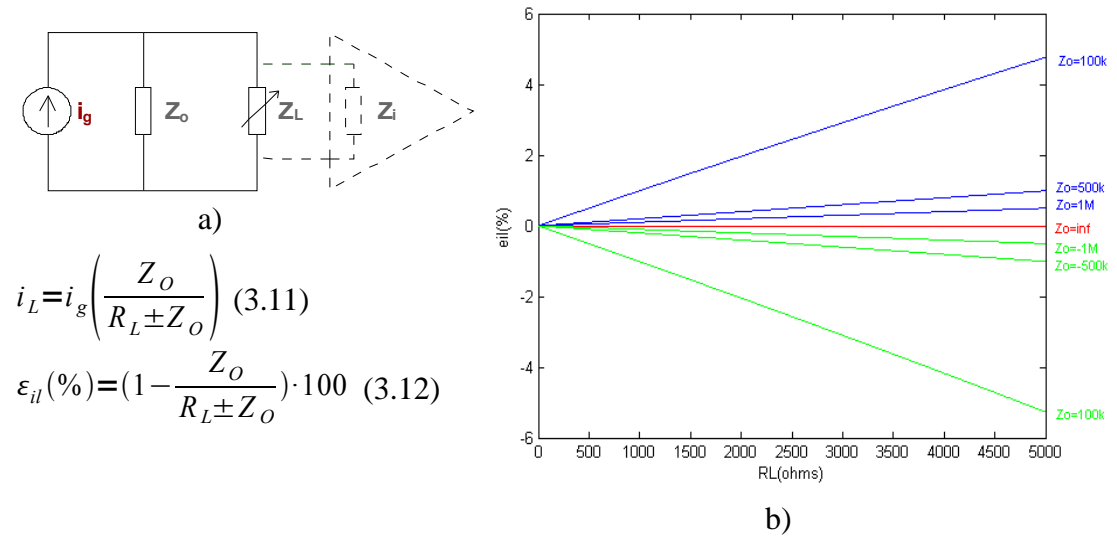


Figure 3.18. a) electronic schema of the non-ideal current source connected to a load. Where I_g is an ideal current source, Z_o the output impedance and Z_L the load. In dashed lines the IA with its input impedance Z_i also connected in parallel. b) Error in the current load depending on the load resistance in the range $[0,5]k\Omega$, for different values of Z_o , in accordance with the formula (3.12) .

The function (3.11) is non-linear, nevertheless if the condition $R_L \ll Z_o$ is kept (it is always fulfilled in this type of circuits), the error is proportional to R_L .

The most logic calibration technique would be to fix a R_L as large as possible and adjust the potentiometer until get $V_L = R_{Lmax} \cdot i_g$, however i_g is neither known. It can be guessed by placing first and other resistance as small as possible, because the error is lower, and use the inverse way $i_g = V_L / R_{Lmin}$.

Theoretically this method is fine to get a low fit, but in practice it has some problems. It is easier to realize watching the direct recorded parameter, it is the voltage depending on the load resistance.

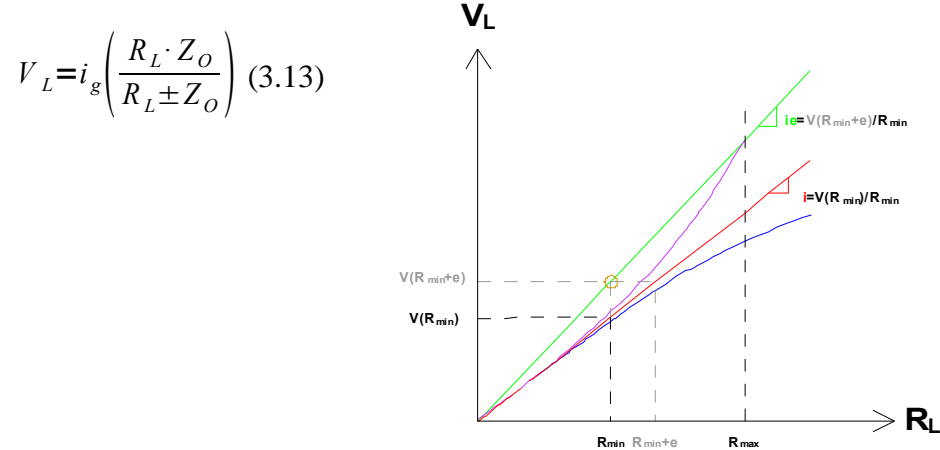


Figure 3.19. Effect of the error in the output impedance calibration, when the current is tried to be guessed by using a small resistance. The red signal belong to the ideal signal when Z_o is infinite, the blue one when Z_o is finite, in green the erroneous ideal signal due to wrong calculation of the slop, and in purple the final wrong signal if the green one is taken as ideal.

As the figure 3.19 shows a tiny error in the i_g calculation, unleash a big error in the output impedance adjust. Moreover this measure is sensitive to the errors in the resistance and in the voltage, the resistance not only has the margin of error but also the input impedance of the measurement devices affects when it is significant, in the voltage case for low resistances the voltage is smaller, thus noise can also hide the signal when it is measured by visual methods as the oscilloscope.

The figure 3.19 is a dramatization of a real case, if the same graph is made the signals are so close that is difficult to difference. However a little trick can be done, it consist of resting the ideal signal to appreciate the error:

$$V_L = i_g \left(\frac{R_L \cdot Z_o}{R_L \pm Z_o} \right) - V_{Lideal}(R_L) = i_g \left(\frac{R_L \cdot Z_o}{R_L \pm Z_o} \right) - R_L \cdot i_g \quad (3.14)$$

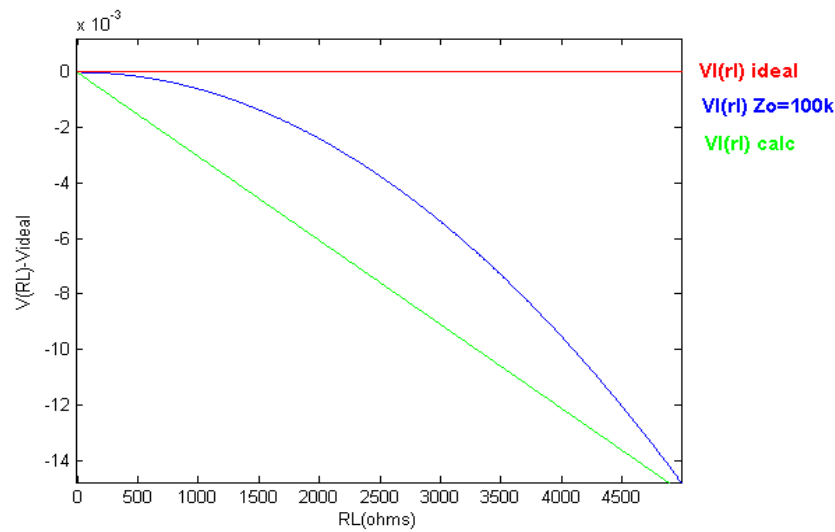


Figure 3.20. Theoretical analysis of the error in output impedance calibration when the $Z_o=100k\Omega$, and the current calculation is made measuring the voltage in a resistance of 100Ω with an error margin of 1%. The red signal belongs to the ideal signal when Z_o is infinite, the blue one when Z_o is 100Ω , in green the erroneous ideal signal due to wrong calculation of the slop.

The previous figure shows how, with this method, even using a 1% range resistance the error is the same that has a output impedance of $100k\Omega$.

An alternative is discussed next. It consists of measuring the current variations by the voltage in a fixed resistance, when the total load is changing. If instead of changing the load resistance under measure a series resistance is placed to increase the

resistive load, the current variation can be obtained independently of this under measure resistance, hence the output impedance could be adjusted to reduce this current changes.

$$V_i = i_g \left(\frac{Z_o \cdot R_a}{R_L \pm Z_o} \right) \quad (3.15)$$

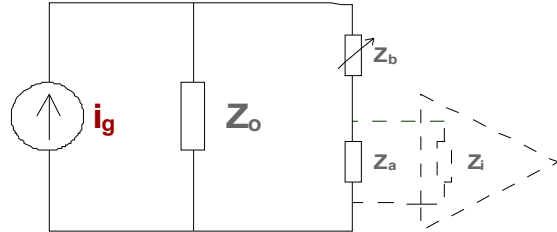


Figure 3.21. Electronic schema of the alternative output impedance calibration circuit. Where I_g is an ideal current source, Z_o the output impedance and the load has been divided in two resistors Z_a and Z_b . In dashed lines the IA with its input impedance Z_i also connected in parallel.

With this circuit the measured voltage becomes proportional to R_a , then the behaviour similar that for the current (figure 3.18.b). Hence unlike the previous method the calibration does not depend on the resistance values, just on the voltage variations between the single resistance and the increased load by adding R_b .

After a qualitative explanation of the method has been done, next a quantitative view is shown. If this calibration technique is review one realises that when the Z_o is trimmed to get a V_o of R_a+R_b equal to the V_o of R_a , the voltage in R_a also changes in a smaller proportion, then V_o of R_a+R_b has to be readjusted, again. This loop should be kept until the output impedance is accurate enough, this point can be known using the formula (3.15) for both voltage measures.

If the two measures are defined as:

$$V_1 \quad \text{when} \quad R_{L1} = R_a \quad \text{then} \quad V_1 = i_g \frac{R_{L1} + Z_o}{Z_o \cdot R_a}$$

$$V_2 \quad \text{when} \quad R_{L2} = R_a + R_b \quad \text{then} \quad V_2 = i_g \frac{R_{L2} + Z_o}{Z_o \cdot R_a}$$

These are equalized by the common terms yielding :

$$Z_o = \frac{V_2 \cdot R_{L2} - V_1 \cdot R_{L1}}{V_1 - V_2}$$

If the voltage difference is defined as $V_d = V_1 - V_2$ and R_L is replace.

$$V_d = \frac{V_2 \cdot R_b}{Z_o + R_a}$$

Where $R_a \ll Z_o$ and $V_2 \approx i_g \cdot R_L$.

$$V_d \leq \frac{i_g \cdot (R_a + R_b) \cdot R_b}{Z_o} \quad (3.17)$$

This formula provides the minimum difference in the voltage to get the wanted output impedance, the resistances precision are not a critic factor here, and the possibility of use a larger resistance to measure the voltage reduces the noise errors.

The configuration chosen to measure this circuit is $R_a = 1K \Omega$; $R_b = 5K \Omega$; and the fixed parameters are $i_g \approx 0.3mA$; $Z_o = 24M \Omega$, then $V_d \leq 75 \mu V$. However this precision is only achievable with a 12 bits device, $V_{dmin} = \frac{V_i}{2^b} = \frac{i_g \cdot R_a}{2^b}$. Hence for the calibration is proposed to use the IA even without has been calibrated, because the wished is not the exact value but the difference.

3.3.2 Gain calibration for a fix frequency

Once the non-linearities have been improved, the calibration becomes much easier, because of the voltage on the load is proportional to the injected current and the voltage measurement circuit gain:

$$V_o = G \cdot V_i = G \cdot (i_g \cdot R_L) \quad (3.18)$$

Where V_i is the amplitude of the signal on the load R_L , V_o is the amplitude gotten after the processing, i_g the amplitude of the current injected signal and G the gain applied to the recorded voltage along the whole process.

This gain is mainly commanded by the IA gain, it is digitally adjustable through a digital potentiometer:

$$G_{IA} = 1 + \frac{49,4 K \Omega}{R_G} \quad (3.19)$$

with R_G controlled as follows:

$$R_G = \frac{D}{256} \cdot R_{AB} + 100 \Omega \quad (3.20)$$

Where D is a 8 bits digital word, and R_{AB} the total potentiometer value, which is about 100K, but it has a 20% margin of error making it as unknown.

Furthermore the IA controlled by D and other factors affects the gain, these are due to the antialiasing filter gain and other attenuation filters or the processing. Then the total factor which multiplies the input voltage can be written as:

$$G(D) = \left(1 + \frac{49,4 K \Omega}{\frac{D}{256} \cdot R_{AB} + 100 \Omega} \right) \cdot G_f \quad (3.21)$$

It is written depending on D , G_f represents the other factors mentioned.

As the formula (3.21) tells the relationship is with D in non-linear and there are two unknown parameters, thus the calibration turns more complicated.

In a first occasion, the calibration was made using curve fitting techniques, by recording a group of points in the equation $G(D)$ and approaching the unknown parameters with the Levenberg–Marquardt algorithm, this way the system was able to use the gain for every value of D . However in practice is more successful to use the same resources to record a number of samples belonging to a D values which produce representative gains.

The D values selection criterion is to take the D values which generate gains close to all possible integers. The table 3.2 shows these theoretical values, when the dependent parameters are fixed at its default values, $G_f = 2$ and $R_{AB} = 100k\Omega$.

Table 3.2. The 30 digital words used and the final gain these produced.

D	Gain	D	Gain	D	Gain	D	Gain	D	Gain
1	x203	7	x36	13	x21	21	x14	42	x8
2	x114	8	x32	14	x19	23	x13	50	x7
3	x79	9	x29	15	x18	25	x12	63	x6
4	x61	10	x26	16	x17	28	x11	84	x5
5	x50	11	x24	17	x16	31	x10	126	x4
6	x42	12	x22	19	x15	36	x9	253	x3

Due to the current is neither known with precision it can be joined to the gain to yields a parameter which provides directly the value of the resistance form the read voltage. Using the formula (3.18).

$$k(D) = \frac{R_L}{V_o} \quad \text{With} \quad k(D) = \frac{1}{G(D) \cdot i_g} \quad (3.22)$$

Then the calibration is done fixing a R_L to 75Ω , because it is the minimum load to do without saturate the IA with the maximum gain (formula 3.18), and recording the value of V_o for every chosen D value to calculate k , the results are stored to use In the inverse way.

$$R_L = k(D) \cdot V_i \quad (3.23)$$

3.3.3 Frequencies dependence correction

The antialiasing filter is also used to double the signal in order to fit the IA output signal, limited by the output swing, into the ADC range. Nevertheless because the filter is not ideal, the gain is not equal in all the bandwidth, it depends on the input signal frequency.

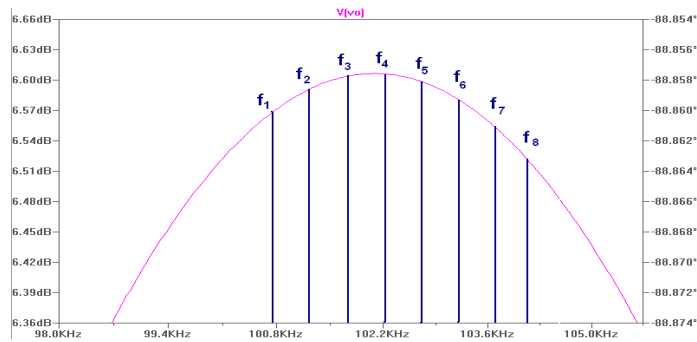


Figure 3.22. Amplify section of the antialiasing filter frequency response together with the eighth frequencies used to test device, in order to show the gain variations depending on the channel.

To adjust these differences, keeping in mind that the set of frequencies are fixed, the variation in the gain for every channel frequency is calculated and stored. One of the frequencies should be chosen as reference and be used to calculate the IA calibration. Then, it is used as base and the gain variation of the others are measured with regard to this one.

$$R_L = k(D, f_b) \cdot \Delta k(f_n) \cdot V_i \quad n = [1, N] \wedge n \neq b \quad (3.24)$$

thus to calculate the variation in the calibration constant depending on the frequency

$$\Delta k(f_n) = \frac{R_L}{k(D, f_b) \cdot V_i} \quad (3.25)$$

Where k is the factor calibration for a digital word D and a frequency f_b chosen as base, Δk the proportional variation in the calibration factor for a frequency f_n , R_L the load resistor, V_i the voltage amplitude of the input signal.

3.3.4 Calibration Procedure

Summarizing, the calibration consists of three steps, for every channel. These calibrations are made averaging a set of final measures to reduce the random errors.

First the adjust of the Z_0 which can be done with the non-calibrated IA, owing to just is necessary check the change, it is done with the resistance values $R_a = 1k\Omega$ and $R_b = 5K\Omega$.

Second to calculate the thirty parameters for $k(D)$, with a $R_L = 75\Omega$, for a frequency chosen as base.

Finally, to calculate the gain variation for the rest of the frequencies with a fix D .

Hence to know the value of the resistance from the measured voltage the relation (3.24) is used.

3.4. Test method

3.4.1 Processing Testing

In order to limit the error sources to the hardware side, good software testing is needed. The whole processing system is described section 3.2.4, it has the aim of filtering the undersampled signals, calculating the envelop and adjusting it to the final output frequency. Hence the input is a sum of eight sinus waves with every of the channel frequencies, and the output the amplitude of one of the sinusoid.

The target of the test is to check the systematic and random errors for all the frequencies, the systematic error must be an offset of the signal which will be rejected by the calibration, and the random error is the samples oscillation around this mean.

The test input consist of the sum of the eight sine waves each one with one of the channel frequencies after the undersampling (table 3.1), and all them with an amplitude of one volt peak to peak $A=1V_{pp}$, a number of samples per second equal to the sample frequency $f_s = 10.000$, and 10 seconds length. This input is applied to a eight channel processing implementation, and the outputs are analysed.

The results are used to study the stability checking if the averages are constant, and the noise, calculating the SNR for different powers of noise in the input, specifically -10dB, -40dB and -80dB. The signal noise ratio is calculated with the formula (3.25).

$$SNR_{f_n} = 20 \cdot \log_{10} \left(\frac{\sigma_s}{\sigma_n} \right); \sigma_s = \text{mean}(V_{out}); \sigma_n = \text{var}(V_{out})$$

Where V_{out} is the output signal.

3.4.2 Calibration Testing

In order to know the effects of the calibration in the measurement, some test are made along all the process.

Gain fixed frequency calibration test

The target of this test is to see the effect on the calibration in the different gains for a fix frequency. The procedure is to measure a resistance for all the gains (table 3.2), and calculate the error regarding the theoretical resistance value, it is made for three resistances of 75Ω , 200Ω , 500Ω and $1k\Omega$. In order to reduce the random errors every sample is calculated as the average of 100 samples.

Gain frequency calibration test

Once the gain calibration has been made for a fix frequency the next step is to calculate the variations for the other channels based on this calibration. To analyze the correct working of it, a sample of every gain (table 3.2) and each frequency (table 3.1) is recorder, for a 75Ω load resistor, and the error is expressed in percentage. The frequency chosen as base is the fourth $f_4 = 102250\text{Hz}$.

Theoretically the error for this resistance should be 0%, in all the cases.

3.4.3 Channel addition effects test

This chapter analyses the effects in the measure when more than one channel is placed in same impedance. A first test checks the dynamic behaviour of the system, to be sure the output is constant for a constant load impedance. A second one observes the static behaviour, checking changes in the final measurement by the channel addition.

Dynamic analysis

This test is similar to the processing test, the difference is the use of real signals. This occasion, there are not eight available signals to inject in the same impedance, there are only three, hence the eight channels can not be measured at the same time. So the solution is to divide what should be one test with eight frequencies at the same time in six tests with three frequencies, the procedure is to test every frequency together with the two neighbour frequencies, it produces the possibility to make six tests as is shown in the next table.

Table 3.3. Distribution of the channel frequencies in each device channel for the six possible tests. Columns define the number of test, and rows the frequencies for every device channel.

	Test 1	Test 2	Test 3	Test 4	Test 5	Test 6
Channel 1	f_1	f_2	f_3	f_4	f_5	f_6
Channel 2	f_2	f_3	f_4	f_5	f_6	f_7
Channel 3	f_3	f_4	f_5	f_6	f_7	f_8

This test does not depend on the precision but on the changes so the gains chosen are not decisive, then it is made for a 75Ω load resistor and x36 gain, and also for 1k and x4 gain. Ideally the output ought to be constant.

Static analysis

After analysing the dynamic behaviour, a study for the changes in the measure is done. The test consists of reading the value of a ten resistors array from 100 to 1k, for all the possible combinations with three channels, considering a channel is made up of a current injector and AI, it means do several records adding the current injectors and or the AI. The set of measures are defined in the next table.

Table 3.4. Definition of the test to do adding the current source and or the IA to a channel. The table group the test for each device channel in three columns also divided in two columns which tell the sources and the IA connected to the load.

Channel 1		Channel 2		Channel 3	
Source	IA	Source	IA	Source	IA
I_1	IA_1	I_2	IA_2	I_3	IA_3
I_1+I_2	IA_1+IA_2	I_1+I_2	IA_1+IA_2	I_1+I_3	IA_1+IA_3
I_1+I_3	IA_1+IA_3	I_2+I_3	IA_2+IA_3	I_2+I_3	IA_1+IA_3
$I_1+I_2+I_3$	$IA_1+IA_2+IA_3$	$I_1+I_2+I_3$	$IA_1+IA_2+IA_3$	$I_1+I_2+I_3$	$IA_1+IA_2+IA_3$
I_1+I_2	IA_1	I_1+I_2	IA_2	I_1+I_3	IA_3
I_1+I_3	IA_1	I_1+I_3	IA_2	I_2+I_3	IA_3
$I_1+I_2+I_3$	IA_1	$I_1+I_2+I_3$	IA_2	$I_1+I_2+I_3$	IA_3
I_1	IA_1+IA_2	I_2	IA_1+IA_2	I_3	IA_1+IA_3
I_1	IA_1+IA_3	I_2	IA_2+IA_3	I_3	IA_1+IA_3
I_1	$IA_1+IA_2+IA_3$	I_2	$IA_1+IA_2+IA_3$	I_3	$IA_1+IA_2+IA_3$

The test is made for each of the three channels, setting the recording channel frequency to f_2 , and the other two to f_1 and f_3 .

3.4.4 Complex Impedances Testing

Along all the testing, the load has been kept pure resistive, however the body electronic model has a capacitive component (figure 2.3). In order to check the working for complex impedances, the device is tested on a circuit with different values which emulates the on body situation. This circuit has the next layout.

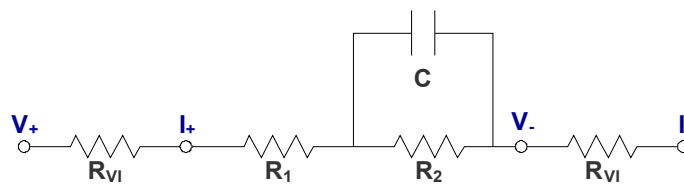


Figure 3.23. Electronic schema of the circuit use in the complex impedance testing. The on blue text indicates the connection points of the device.

Where R_{v1} represents the resistance in between the electrodes it is 50Ω for all the cases, and R_1 , R_2 and C , have different values for every test circuit, these values are written in the table 3.5. The resistivity of a capacitance can be obtain by using the formula (3.26), thus the total resistive load can be calculated by the formula (3.27). All these components have a error margin of 1%.

$$X_c = \frac{1}{2\pi \cdot f \cdot C} \quad (3.26) \quad R_{eq} = R_1 + R_2 \parallel C \quad (3.27)$$

To realize the test, the device is setted with a fixed configuration, $f_{ch1}=f_1$, $f_{ch2}=f_2$ and $f_{ch3}=f_3$. And to get a highest precision every channel is calibrated for its working frequency, hence the frequency calibration errors disappear. The next table shows the value of the variable components and the value these produce for each of the chosen frequencies.

Table 3.5. Definition of the complex impedance tests. The table shows the columns the components of the circuit values, and the real values these produce for the different frequencies used.

<i>N° Test</i>	<i>R₁</i>	<i>R₂</i>	<i>C</i>	<i>R_{eq} for f₁</i>	<i>R_{eq} for f₂</i>	<i>R_{eq} for f₃</i>
1	309Ω	182	220nF	309.3	309,3	309.3
2	475	442	100nF	475.8	475.8	475.8
3	301	953	68nF	302,4	302,4	302,4
4	133	243	22nF	166,4	166,1	165,9
5	475	442	10nF	534,9	534,4	533,8
6	120	953	10nF	212,3	211,6	210,9
7	82	27	68nF	94,7	94,6	94,5
8	180	243	10nF	276,1	275,5	275
9	324	953	3.3nF	644	642,1	640,2

3.4.5 On body testing

Finally an on body test is made. This test is more qualitative than quantitative, it means that the purpose is just to test the device in real conditions and check the right working.

To make the test electrodes are placed in the thorax in a way the signals cross the lungs. Every channel has four electrodes these are grouped in pairs, one for the current injection and the other for the voltage recording, each pair is setted in an opposite location of the thorax, the concrete potions are shown in the pictures (figure 3.24). In addition in order to have an independent reference with to compare the lungs changes a spirometer is used at the same time.

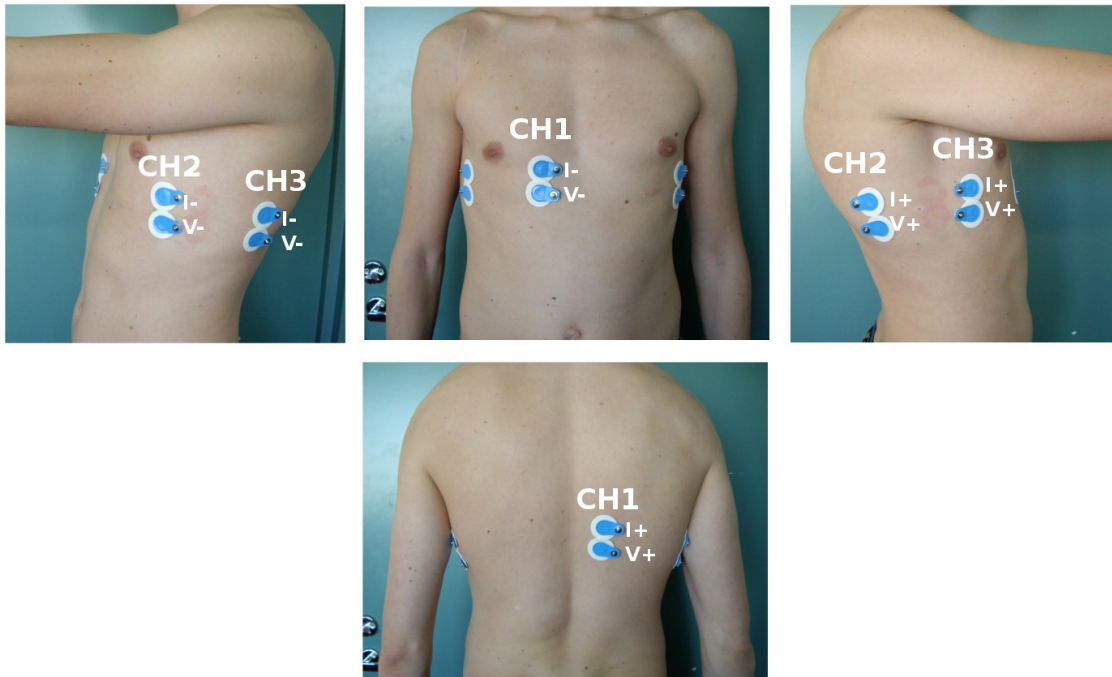


Figure 3.24. Location of the electrodes around the thorax in the on body test. The text indicates the channel which the electrodes belong, and the device connexion agree with the tetrapolar configuration.

The procedure consist of recording every channel alone, two channels together and finally the three at the same time. The measures are made on a standing man breathing normally along one minute. For all the test also the spirometer signal is recorded in parallel.

The sample analysis is made using the spirometer signal as reference. The parameter to compare is the amplitude of the breathing peaks, for every peak is calculated the quotient between the amplitude in the spirometer signal and in the bioimpedance signal, this provides a relation factor for each peak. These are averaged to get a relation factor of whole the signal. Hence the aim of the test is compare this factors, these should be equal for each channel even with the channels addition.

The calculation of peaks amplitude is made by a program which to find the maxima and minima in the signal, and to rest to the maximum the mean between the two minima adjoining it. It is explain in the next figure with a real piece of the one bioimpedance signal as example.

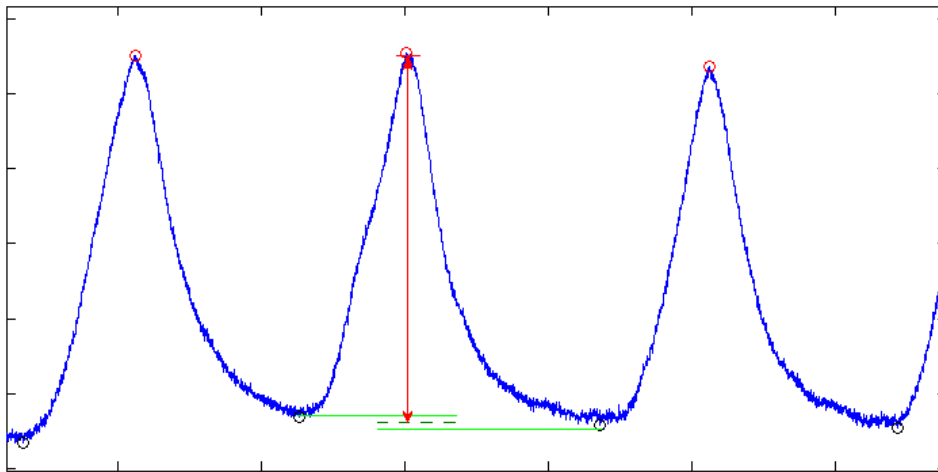


Figure 3.25. Amplitude calculation method. The program detects the maxima , these are indicated with red circles and the minima with black circles. It uses the mean between the neighbours minima, on green dashed line, as base of the signal to calculate the amplitude represented by a red arrow line.

4. Results

4.1 Processing testing

The table 4.1 shows the results of the processing test explained in the section 3.4.1. It belongs with the SNR in the input for different noise powers.

Table 4.1. Signal noise ratio for every output for different noise power at the input. Columns show the SNR at the output for noise power at the input in every row.

σ_n	SNR _{f1}	SNR _{f2}	SNR _{f3}	SNR _{f4}	SNR _{f5}	SNR _{f6}	SNR _{f7}	SNR _{f8}
-10dB	19.19dB	19.69dB	19.80dB	19.24dB	19.52dB	19.23dB	19.95dB	19.61dB
-40dB	48.64dB	48.12dB	48.21dB	48.38dB	47.66dB	48.26dB	47.87dB	48.73dB
-80dB	88.62dB	88.27dB	88.48dB	87.58dB	88.23dB	88.57dB	88.75dB	87.63dB

The differences between the outputs are small and random, the improvement of the noise in 8dB regarding the input noise is due to the averaging of the signal every final output period.

4.2 Calibration Testing

4.2.1 Variable Gain Fix frequency

The next chart shows the error in %, for three resistances of 75Ω , 200Ω , 500Ω and $1k\Omega$, measuring, depending on the gain.

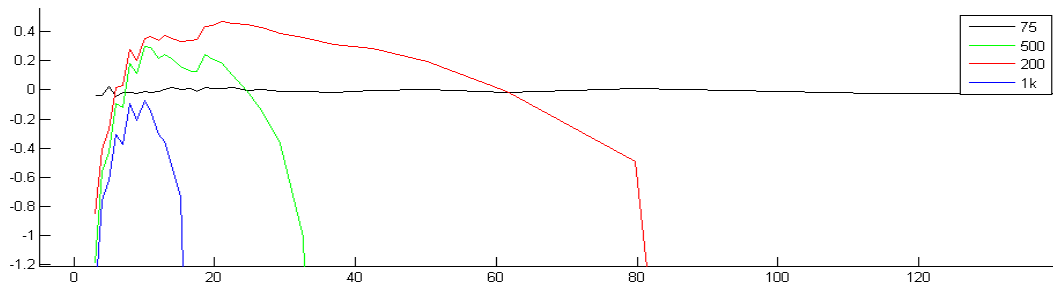


Figure 4.2. Error depending on the gain, horizontal axes defines the gain, and vertical axes the error in percentage. The chart shows results for different resistive loads, on black for 75Ω , red for 200Ω , green for 500Ω and blue for $1k\Omega$.

For the 75Ω resistance the error is almost zero because of that is the calibration value. The errors for low gains are due to the calibration, at this gains the SNR is too small for the 75Ω calibration resistance, the signal is confused with the noise. The error at higher gains is owned to the saturation of the amplifier, for large resistances. The offset error is produced by the 1% resistances error margin.

4.2.2 Variable Gain Variable Frequency

Analysis of the error in percentage in a 75Ω resistance measurement, for every gain (table 3.2) and each frequency (table 3.1). It is shown in a 3D plot where the X axis is the eight frequencies, the Y axis the thirty gains from the highest to lower as are written in the table 3.2, and the Z axis the error. To make the reading easy, also two lateral views are shown, the right one is the error depending on the frequencies, and the below one depending on the gain.

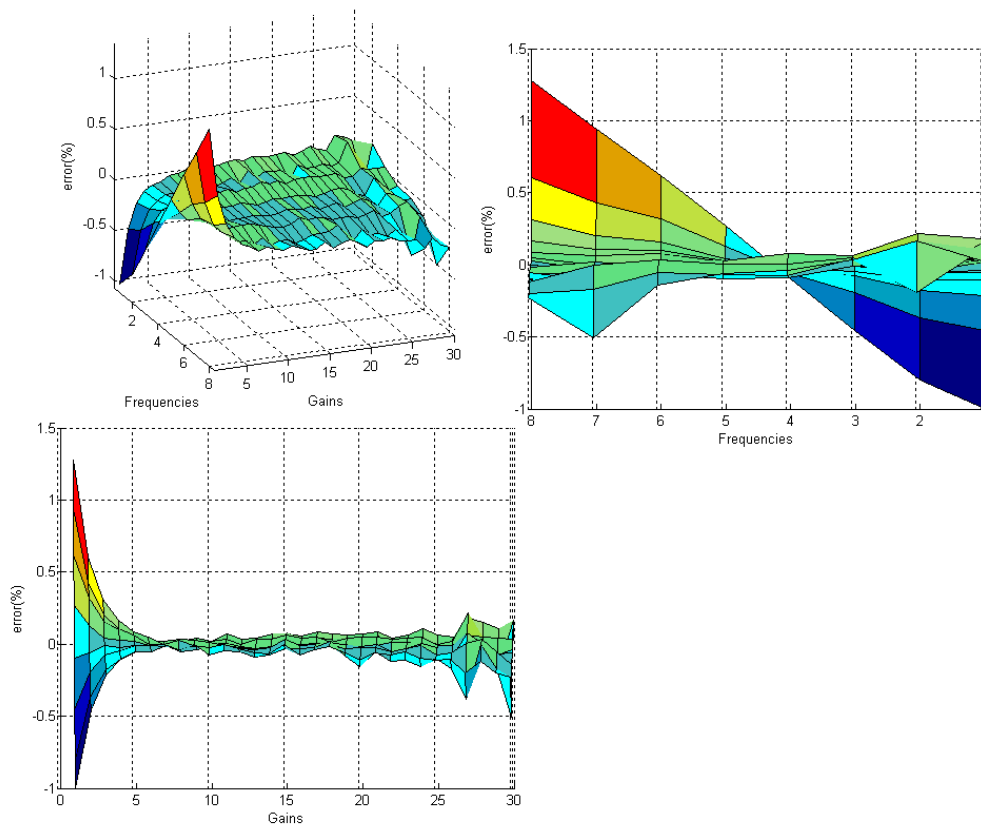


Figure 4.3. Relative error depending on the gain and the frequencies. In the 3D chart the X axis define the eight frequencies, the Y axis the thirty gains from the highest to lower as are written in the table 3.2, and the Z axis the error. For a better reading two lateral views are attached, the right one shows the changes from the frequencies view, and the lower one from the gain side.

The results are not the expected, for the parameters used in the calibration, the fourth frequency and the x36 gain (number 6 in the chart), the error is about 0%, however the error for gains above the used as base are rather huge, until 1% for the more distant frequencies. This mismatch has been examined to conclude that it is due to the IA limitations, if the IA limitations are analyzed, the amplifier has a non lineal gain with the frequency when these are upper x100 and 100Hz. Then the only solution is to find an other IA able to work for these ranges. Or to fix a frequency for every channel, turning it more rigid.

4.3 Channel addition test

4.3.1 Dynamic analysis

The next charts are the three outputs of the device along thirty seconds for a resistive load of 75Ω , the abscissas are the time in seconds and the weights the error in percentage.

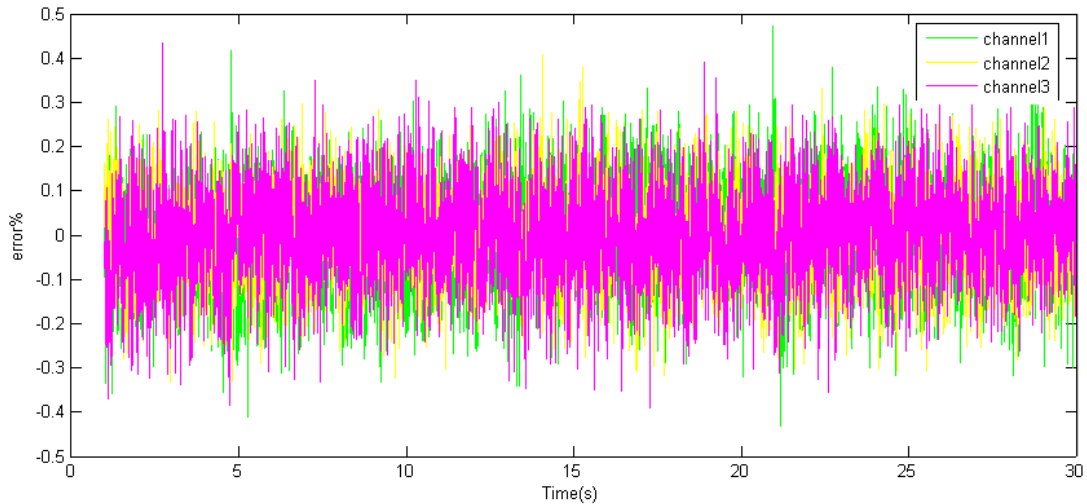


Figure 4.4. Relative error in the output for the three device channels when these are connected to a same load along thirty seconds. The frequencies for each channel in this chart are $f_{ch1} = f_1$, $f_{ch2} = f_2$, $f_{ch3} = f_3$, and the signals belonging are green for the channel 1, yellow for the channel 2 and magenta for the channel 3.

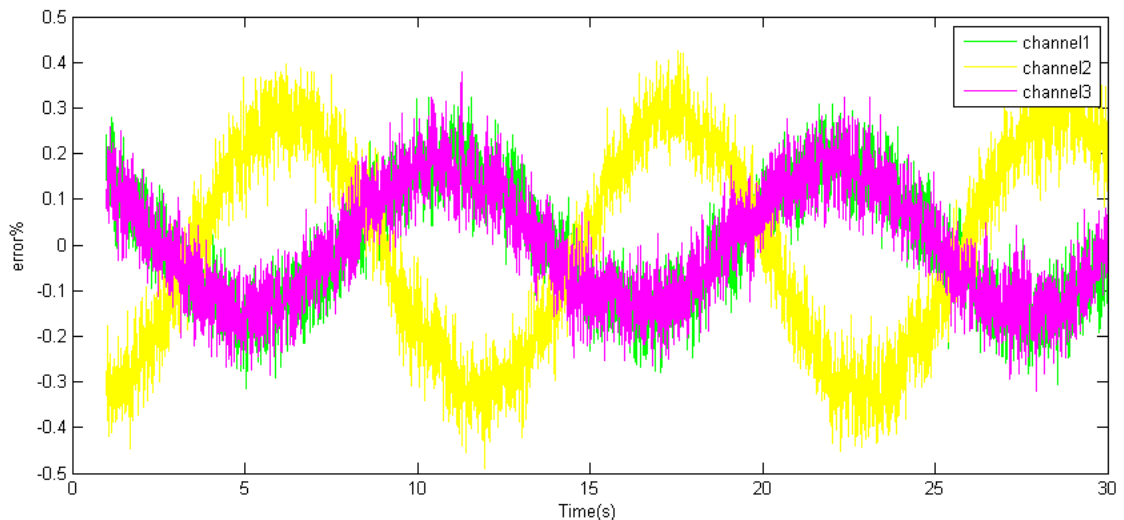


Figure 4.5. Relative error in the output for the three device channels when these are connected to a same load along thirty seconds. The frequencies for each channel in this chart are $f_{ch1} = f_2$, $f_{ch2} = f_3$, $f_{ch3} = f_4$, however the results are similar for all the others combinations of the table 3.3. The signals are on green for the channel 1, yellow for the channel 2 and magenta for the channel 3.

The results are a little strange, for the first combination, with the frequencies f_1 , f_2 and f_3 , the output is the expected as the figure 4.4 shows, however for the rest of the combinations appear a signal error of 0.4% in amplitude and 0.1Hz.

It should be due to the non idealities in the sinus wave generated by the DDS, the signal is not a pure sinusoid, and in the frequency spectrum it has harmonics together with the main signal. However the error does not appear for the lower frequencies, may be because of the harmonics distribution, it should be study deeper to find the right combination to remove or decrease this error.

4.3.2 Static analysis

This section discusses the results of the static test, it consist of measuring the value of ten resistances, for different combinations of connexions to the load between the current injectors and IA of the three channels. The way to show the results, is concerning to the relative errors, all the measures are made relative to the resistance value in order to remove the errors due to the resistance mismatches, the results of the single channel (the current source and the AI) are kept as base and the other errors are shown with regard to it.

Hence the graphs have in the horizontal axes the ten resistive load values, and in the vertical axes the increment in the error regarding to the one channel error.

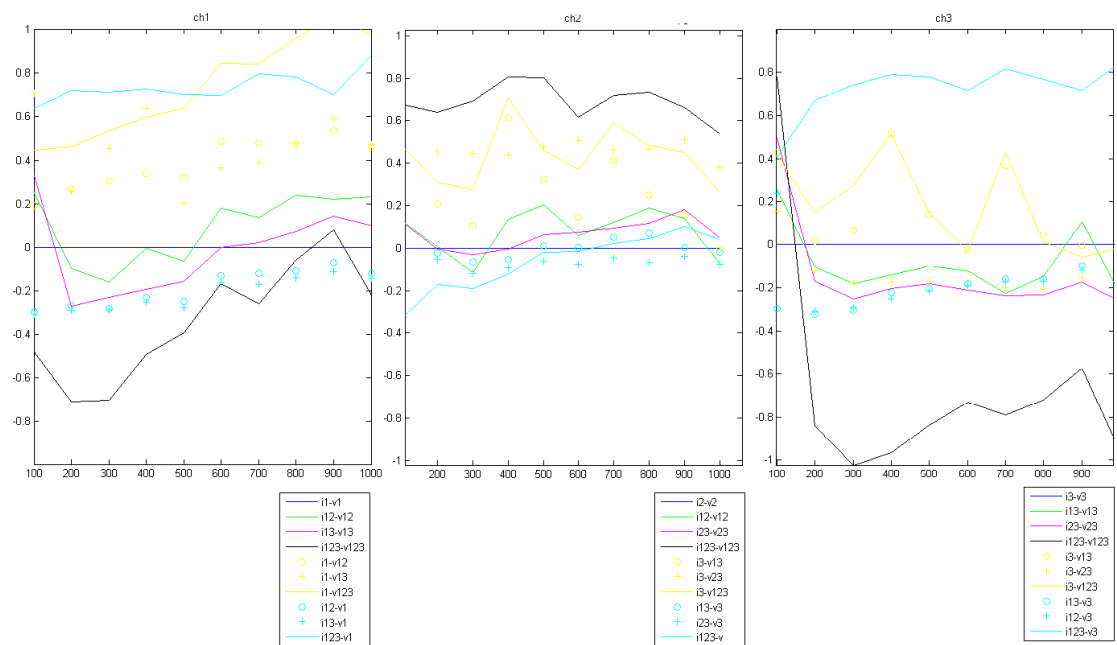


Figure 4.6. Changes in the relative error with the components addition. The three charts show the variations in the relative error with regard the single channel errors for different load resistors. Every chart belongs to a channel as recorder, and the graphs are defined in the legend with a code which tells the current sources connected

preceded by an “i” and the IAs by a “v”. The cyan draws are the possible current additions for a fixed IA, and the yellow group the IA possibilities with a constant source. On green and magenta the connection of one whole channel (current source and IA), and on black all connected.

Theoretically the error should increase with the addition of components and be higher for the larger resistances, because every element adds a parallel resistance, however this effect is hidden by others. The results are difficult to understand, on one hand if the effects of IA addition are analysed look as a positive and random increment in all the cases it could be due to the noise growth. In the other hand the addition of one current source is not decisive in any case, but the placement of three shows a high increment for the first and third channels. It also happens when the analysis is made adding the pair current source and IA. This error must be understood better owing to it can turn harder with more channels.

4.4 Complex Impedances

Here the result of the complex impedance test, the tables shows in the rows the test and in the columns the results of each channel and the gain used in the records. The gains has been chosen to get the maximum amplitude in the signal.

Table 4.2. Result of the complex impedances test, rows indicate the test number and in the columns the results of each channel and the gain used in the records.

<i>Nº Test</i>	<i>Channel 1</i>	<i>Channel 2</i>	<i>Channel 3</i>	<i>Gain</i>
1	311,4	309,1	311	x10
2	474,8	474,4	473,9	x8
3	302,2	301,5	301,9	x8
4	166,7	165,8	165,9	x14
5	536,1	532,9	534,1	x7
6	210,1	208,6	209,1	x12
7	94,8	95,4	94,9	x36
8	274,1	272,5	272,6	x12
9	622,7	614,5	617,43	x6

The results are the expected, the errors are due to the other limitations mentioned, as the calibration errors.

4.5 On body analysis

Next table shows the relation factors explained in the section 3.4.5. The rows contain the factors for each channel, for the different test defined in the columns. These are an individual test, a test with two channels and a the three channels test.

Table 4.3. Relation factors between the spirometer signals and the bioimpedance signals. Rows show the recording channel, and columns the channels connected to the body.

	<i>Individual</i>	<i>Channels 2 and 3</i>	<i>Channels 1, 2 and 3</i>
Channel 1	0.5788		0.6517
Channel 2	0.3143	0.3267	0.3819
Channel 3	0.2747	0.2899	0.3112

The results looks rather bad, however along the processing was observed the method is influenced by the noise, and the factors in every peak are quite different each others.

Anyhow there is an increment in the factors with the channel addition, it has been also seen in the static analysis.

5. Conclusions

5.1 Achievements

Along this document the possibility of building an efficient and accurate multichannel bioimpedance measuring device has been proved. The research about to seek the most suitable method for the bioimpedance multichannel measurement has yielded to a smart frequency multiplexing system with digital undersampled demodulation which provide an encouraging features such as the flexibility, scalability, modularity and simplicity. The implementation of a test device has proved the main theoretical ideas and it has revealed some limitations which were not found in the theory. Finally the on body test has demonstrate that the device can be use for the real original target without produce interferences between the channels.

5.2 Errors and Improvements

As the previous section mention the aim has been achieved successfully nevertheless some problems and possible improvements have been found, ones due to the circuit limitations are easy to solve, others were not expected in the theory thus need a deeper study. This section summarizes these and proposes solutions.

Current Source Output Impedance Calibration

The output impedances calibration of the Improvement Howland was decided to be fixed by hand, in order to remove the problems produced by these in the channel addition. However for a serious device it should be self-calibrated, to reduce the fabrication problems. One way could be replacing the manual method for and automatic one which keeps the same rules, but the best option should be a good study of the possibility of joining this to the main calibration by using a three points self-calibration method[17], all this having the channel addition effects in mind. Furthermore for a whole impedance measurement, it means including the imaginary part, the output capacitance must be also calibrated by using a NIC or a GIC as the section 2.2.4 explains.

Gain Calibration

The problems in the gain calibration are mainly related with the IA. It has a important limitation, the gain changes depending on the frequency when the gain is over $\times 100$, it makes difficult the calibration for the different frequencies. It does not matter if for a final device with fixed frequencies per channel, as in the body test, however is a easy solution problem to get a more configurable device. In addition the IA gain controlled by the digital potentiometer is non-linear, doing the calibration really annoying. The solution should be find an other IA or to use a custom-made one.

Processing

In this development the processing has been made by a laptop, however in possible future device implementations using a microprocessor the software load should be analysed, especially for the envelope detection. The Hilbert transform is to slow, a study for the best compromise speed versus SNR should be done. Some alternative ideas are, applying techniques well-know in the AM area, or dedicate algorithms [22]. This configuration might be modified or improved in case of want the imaginary part.

Channel addition

As has been said in the results, the addition of channel produces on one hand a dynamic error, and on the other hand a static error.

The overlap of the low frequency signal is due to the harmonics in the DDS generated signal, an analysis to know the harmonics location after applied the undersampling would solve this problem replacing the channel frequencies.

The constant behaviour with the channel addition also must be study deeper, when more channels are added. This research goes together with the self-calibration.

5.3 Future Work

This thesis represents a first approach to develop a multichannel bioimpedance measurement device. This study has been really useful to establish the bases, prove the correct working of the ideas and find unexpected troubles, but it is not enough to build a good quality system. This section provides a look to the future in order to develop a improved device.

First of all, would be good think about the target towards the development should go. The innovation of the system makes difficult to find a specific application where focuses the aim, it provides a lot of use possibilities, some still unknown. Because of this and the mentioned flexibility and scalability properties, is proposed to channel the development towards an objective open to all kind of applications.

The easiest and secure choice to build a flexible system would be by creating independent configurable modules. Every module would be an individual bioimpedance measurement block make up of a current injector, a voltage recorder and a processing unit. These should be calibrated, would be able to read all the channels with the maximum amplitude and would leave to configure the frequency and amplitude signal output, the number of channels to read and the sampling and output frequencies. A chosen number of modules could be managed by a main unit process, this configuration distributes the software resources then the main process unit could be fully used to operate the read bioimpedances data in order to get whatever final measure. The configurable modules would leave also the better use of the limited resources as the maximum injected current or the frequency spectrum.

The main advantages of the modules are the independence and modularity, once the modules have been designed will be easy to create a number of these, with the confidence that these are working, it reduces the building and testing processes if it is compared with a fixed structure. In addition one more time the advantages of flexibility and scalability appear the modules can be used for a concrete application without the necessity of making a custom circuit for it, and more channels could be added if is necessary without rebuild the circuit. It provides the chance to test possible applications, and when these work properly to start a custom design if it needs especial features such as size or consume.

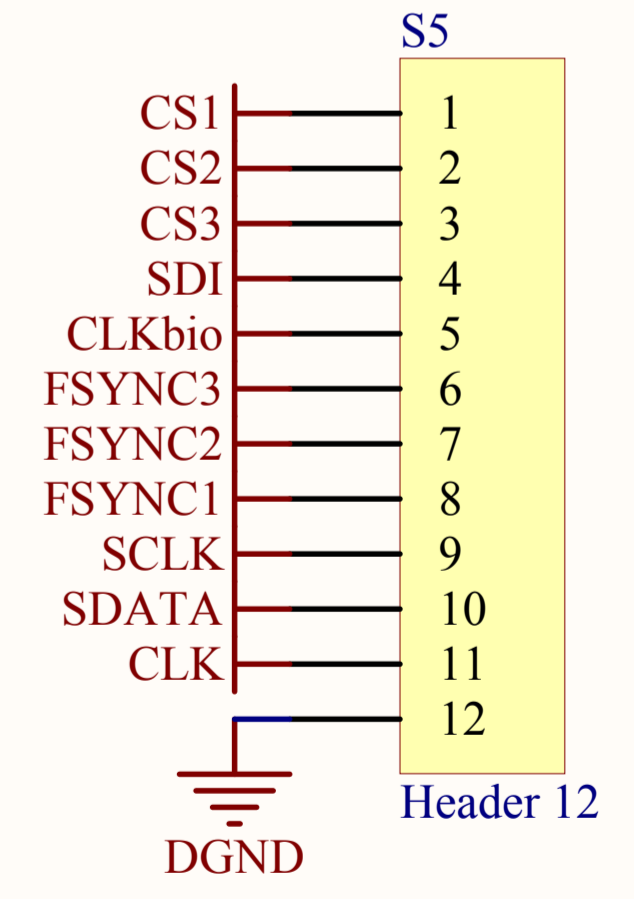
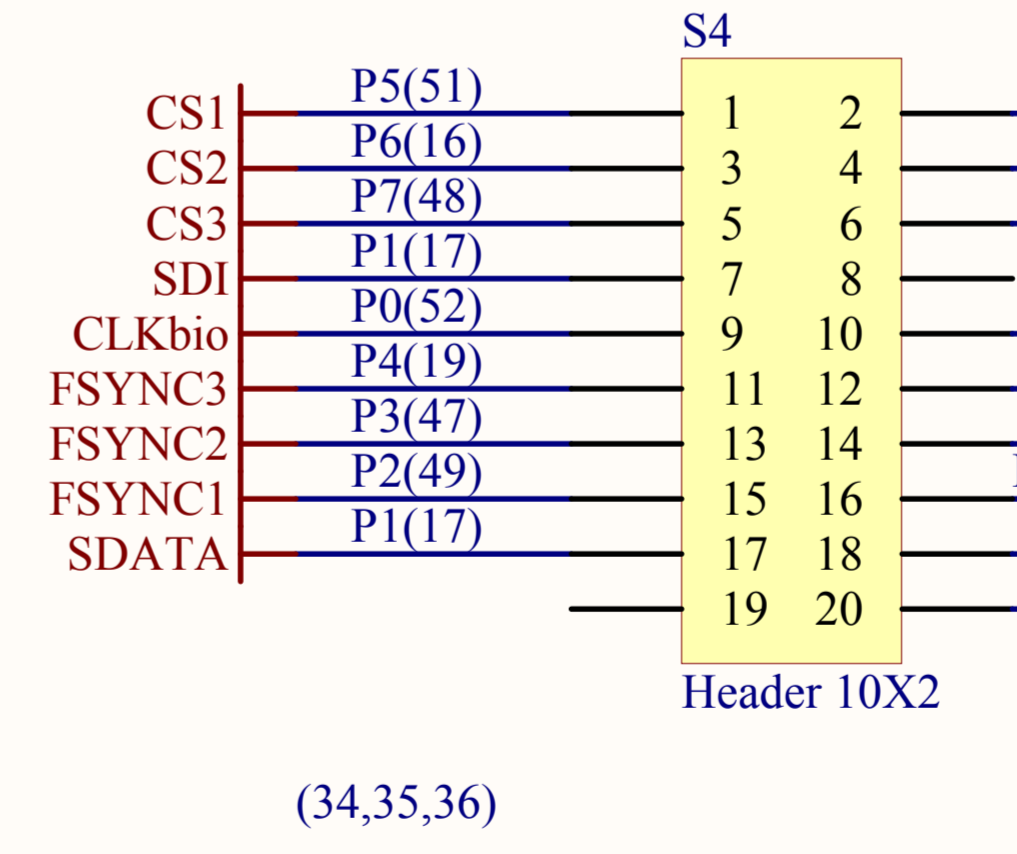
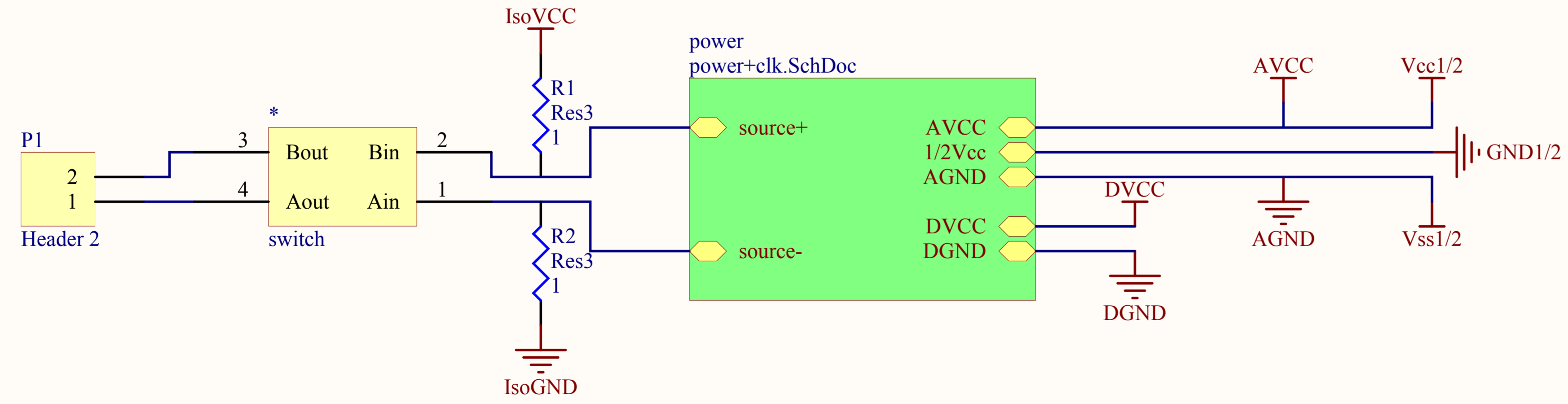
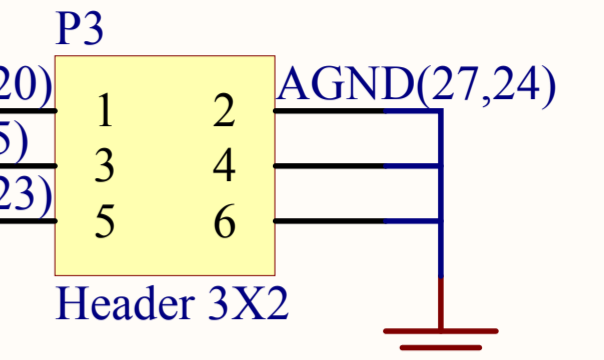
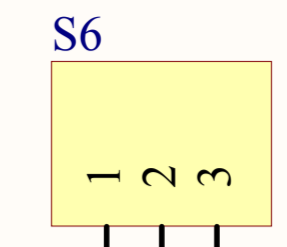
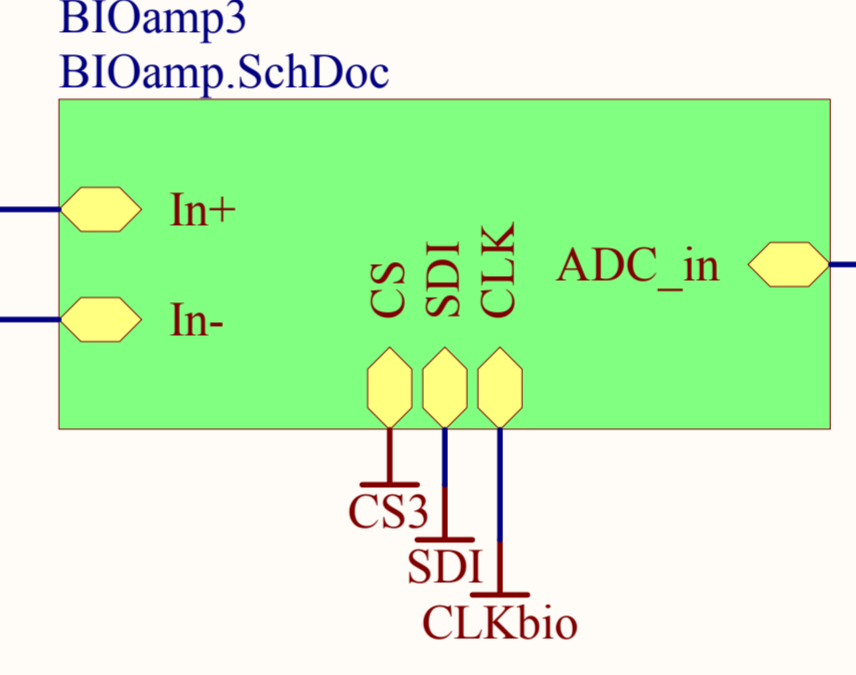
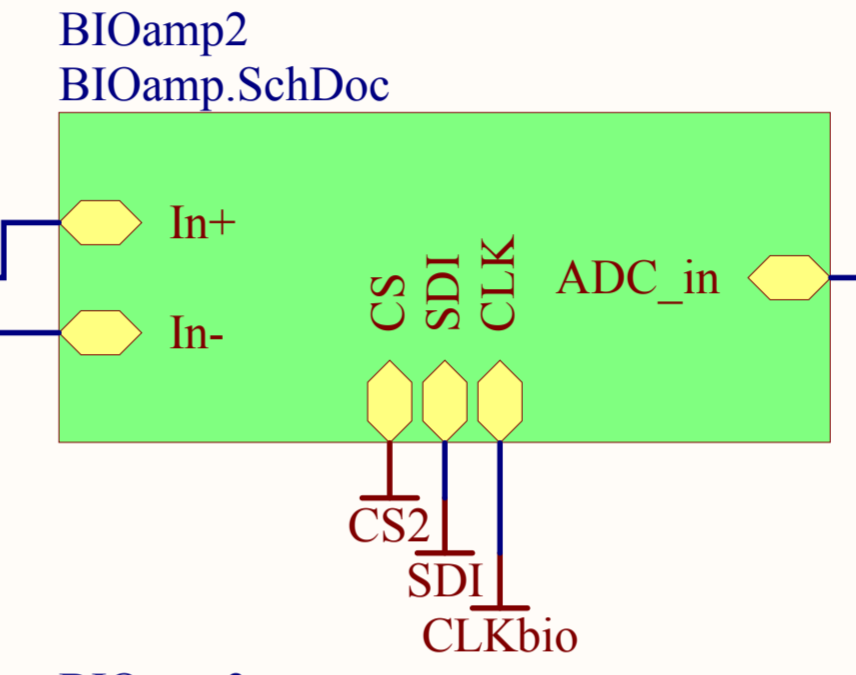
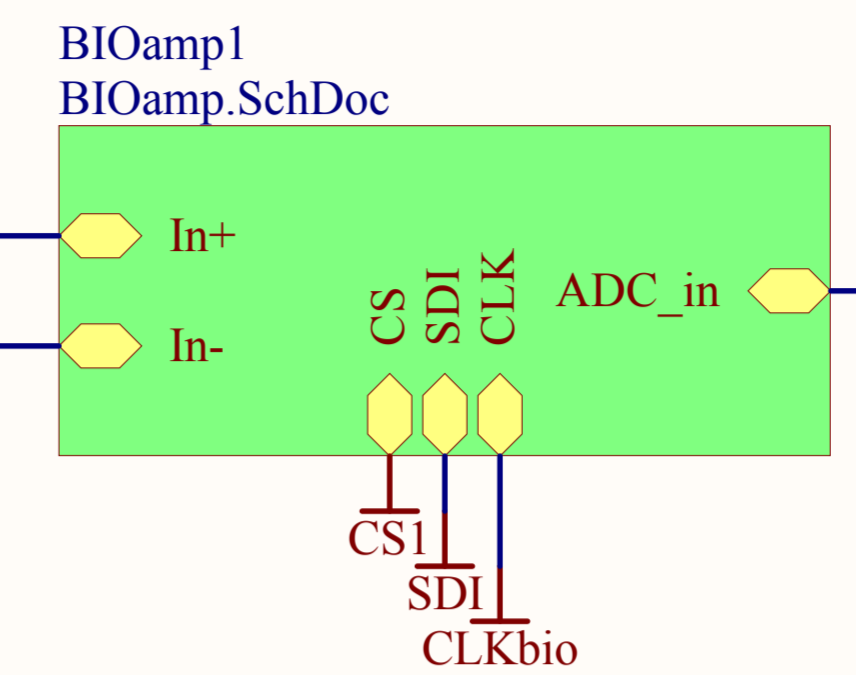
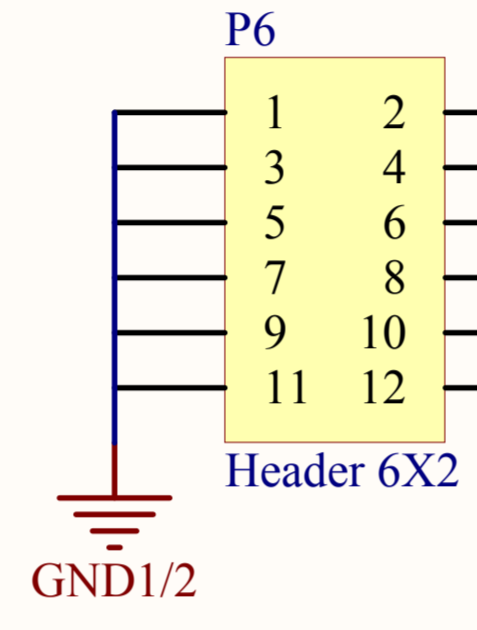
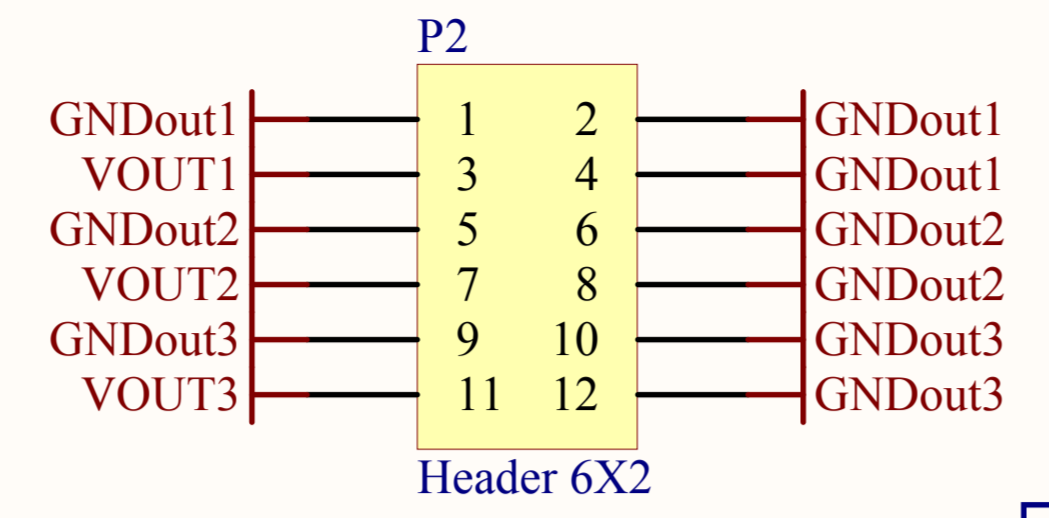
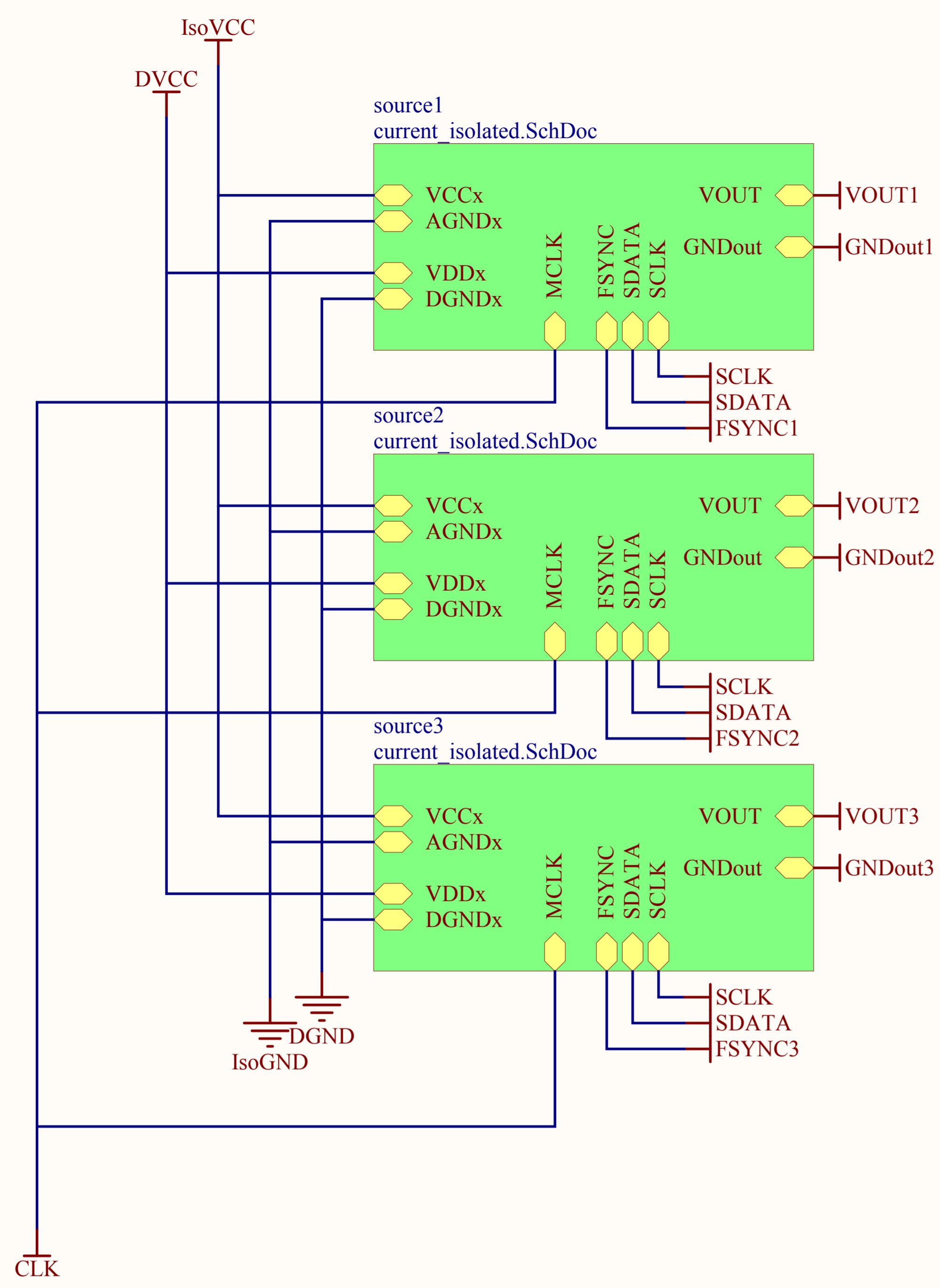
The way to face up this development could be dividing the problem in three research paths, one focused in the analog part, an other in the processing and the third one to investigate concrete applications. In the analog side a deeper study must be done, first to understand the behaviour of the current sources addition in a low level (OpAmp level), second to find all the possible transconductance amplifier circuits and output impedance calibration methods, to do a theoretical study (specially for the self calibration methods), third to check by simulation the most promising configurations and fourth to test in practice the best working ones. For the processing and digital part, first the problem with the harmonics must be solved, next would be needed a study of the possible techniques to get the amplitude and phase of the signal thinking specially in the computational load and in the best platform to implement this, between uProcesor, FPGA, DSP or SoC. Finally the research of applications should be the most important because it is going to give a meaning to the device, some of these can be already tested using the developed prototype.

An idea to proceed could be to separate the analog part from the digital part in the modules implementation, it means to build a module makes up of two boards, one for the current injector and the other one for the rest joined by connectors. It would make easier not only the processing unit test but also the in practice test for different current sources configurations. Hence should be a good idea start designing the digital side, to build some of this processing blocks, and to use these to try test the analog research.

References

- [1] WEBSTER, J. G. “*Medical Instrumentation: Application & Design, 3rd ed*”. John Wiley, 1998.
- [2] Ville-pekka.
- [3] S.Grimes and Ø.G.Martinsen. “Bioimpedance & bioelectricity, basics”. Academic Press, 2000.
- [4] “Introducción a la Bioingeniería”. Marcombo, 1988. (serie Mundo Electrónico)
- [5] Camela Gabriel, sami Gabriel. “Compilation of the dielectric properties of body tissies at RF and microwave frequencies”. King's College London ,1996.
- [6] David S Holder. “Electrical Impedances tomography, Methods, History and aplications”. Institute of Phisics, 2005.
- [7] Allan F. Pacela. “Impedance Pneumography – a surver of instrumentation techniques”. Med. & biol.Engng Vol4. Perganton Press, 1966.
- [8] K G Boone and D S Holder. “Current approaches to analogue instrumentation desing in electrical impedance tomography”. University College London, 1996.
- [9] W Wang, Mbrien, D-W Gu and Yang. “A Comprehensive Study on Current Source Circuits”. 13th International Conference on Electrical Bioimpedances, 2007.
- [10] Robert A Pease. “A Comprehensive Study of the Howland Current Pump”. National Semiconductors Aplication note 1515, 2008.
- [11] Sergio Franco. “Design With Operational Amplifiers and Analog Integrated Circuits 3^oEd”. McGraw-Hill, 2002.
- [12] Hongwei Hong, “Floating Voltage-Controller Current Sources for Electrical Impedance Tomography”.IEEE 2007.
- [13] Jerry Steele and Tim Green. “Tame Those Versatile Current-Source Circuits”. Apex Microtechnology Cor, 1992.
- [14] José E. Mizeño Marquez. “Pricipios de las comunicaciones”. ULA 2005.
- [15] Teodor Neagoe and Robert Fugerer. “Sampling and Reconstruction of Periodic Signals”. DSP-FPGA.
- [16] “Putting Undersampling to Work”. Pentek Tutorials. Pentec, Inc.
- [17] Ji-Gou Liu, Uwe Frühauf, Andreas Schönecker “Accuracy improvement of impedance measurements by using the shef-calibration”. Elsevier Science Ltd, 1999.
- [18] “LMV721 datasheet”. National Semiconductors 2008.
- [19] “AD8221 datasheet”. Analog Devices, 2008.
- [20] “AD5165 datasheet”. Analog Devices, 2008.
- [21] Alan V. Oppenheim, Ronald W. Schafer. “Discrete-Time Signal Procesing”. Pretice-Hall International, 1989.

Apendix A : Prototype Device Electronic Schematics



Title		
Size	Number	Revision
A4		
Date:	11/06/2009	Sheet of
File:	G:\ESTUDIOS\...\Global.SchDoc	Drawn By:

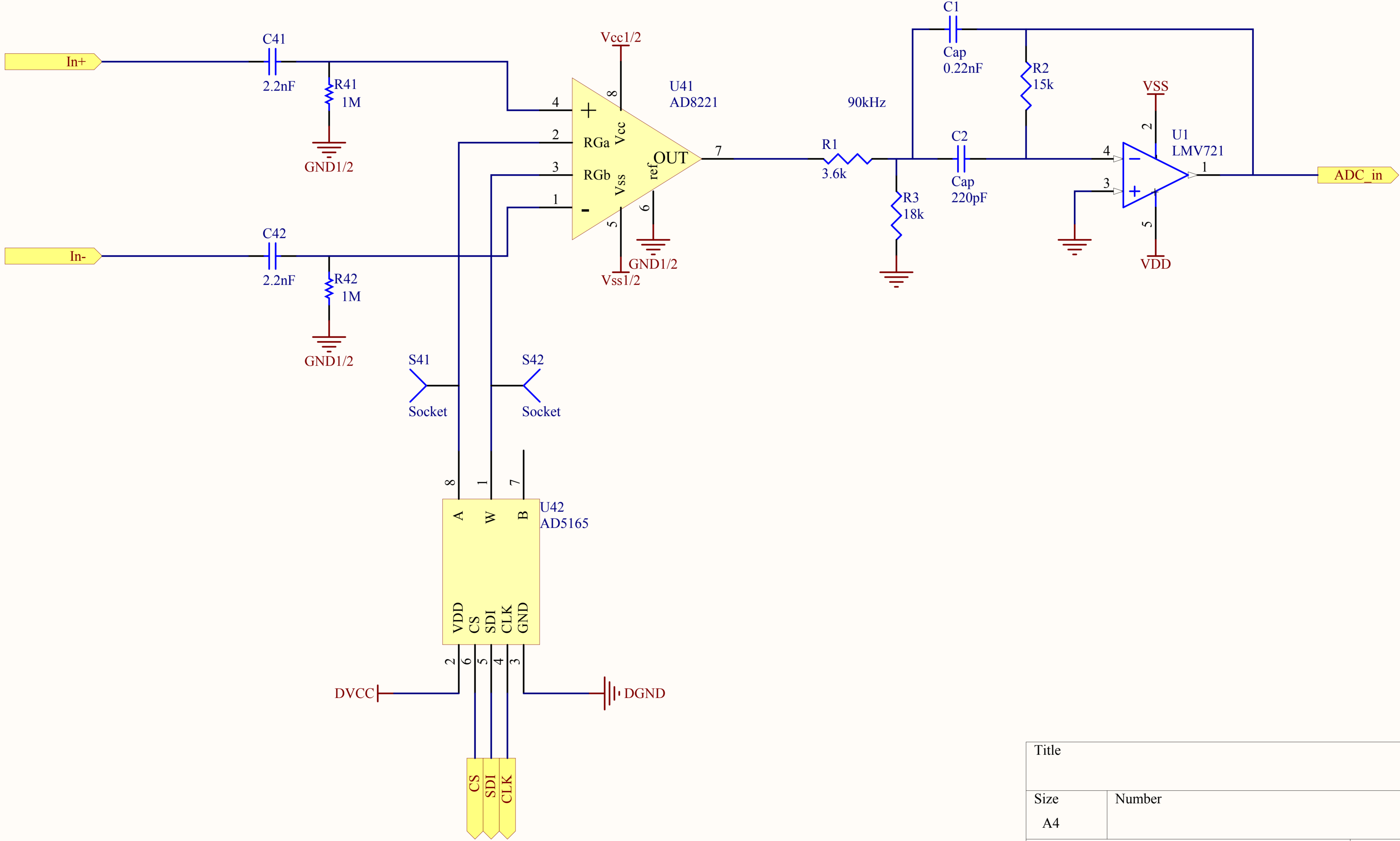
Antialiasing filter + swing amplification

Fo=106kHz G=2

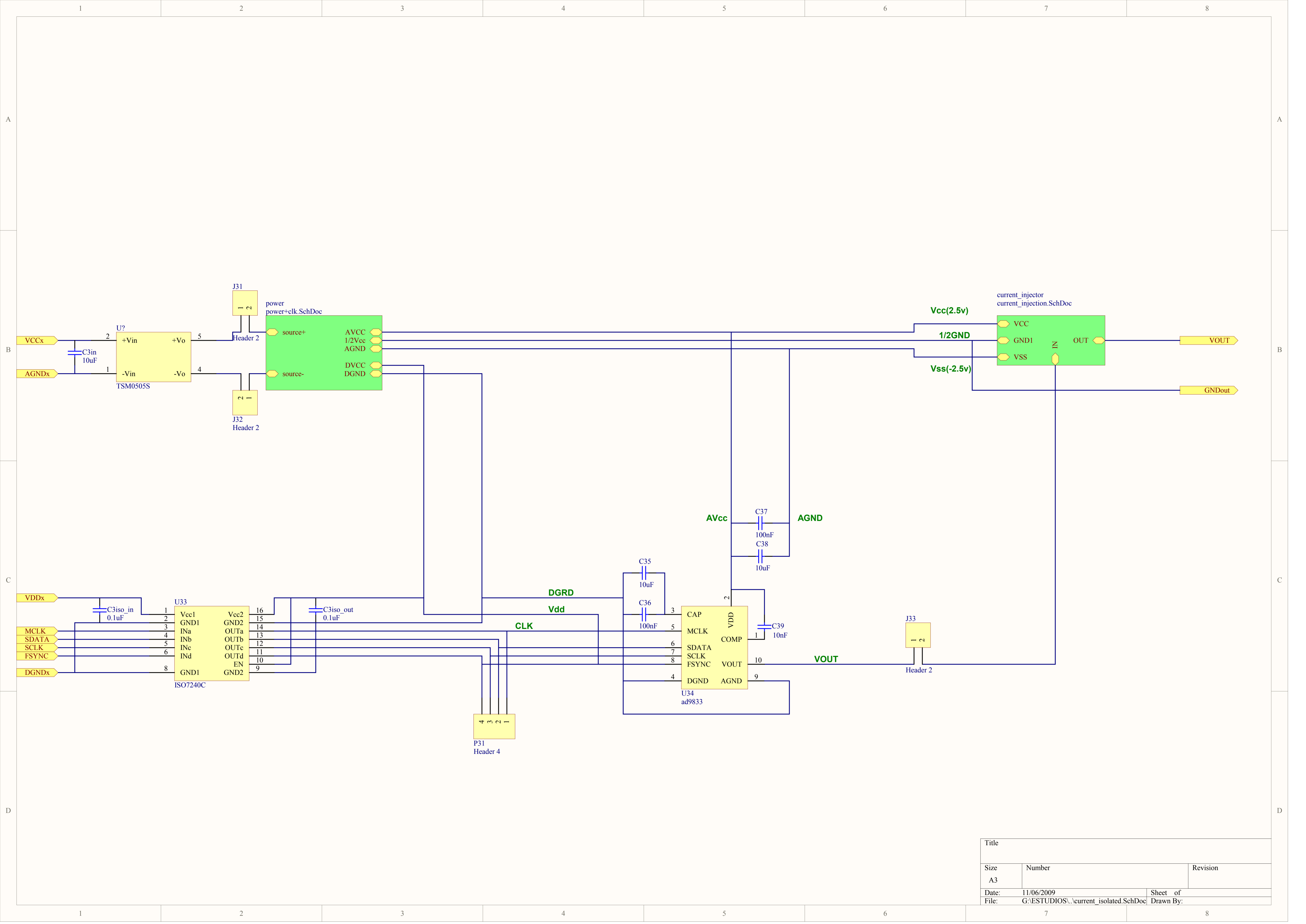
-3dB @ [68,167]KHz
-1dB @ [81,140]KHz
-33dB @ [100,116]KHz

Ibias_paht(F<72Hz)

R=1M to reduce the paralel resistance with the current injector



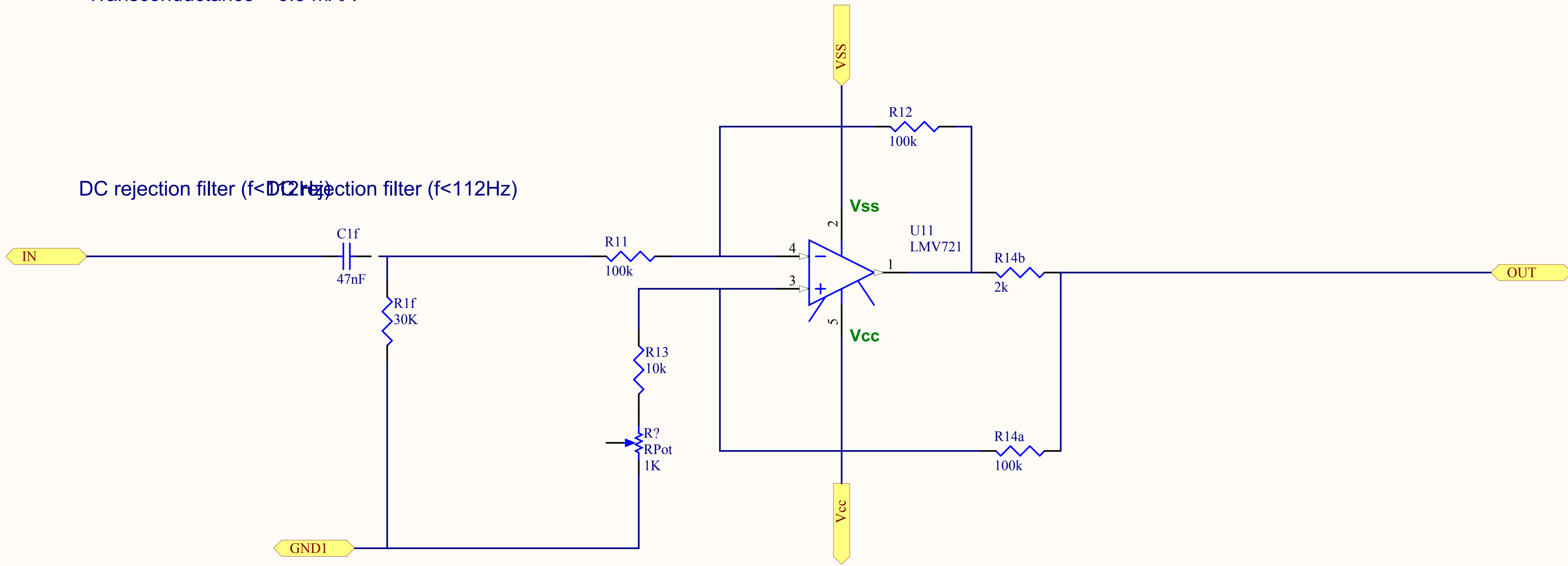
Title		
Size	Number	Revision
A4		
Date:	11/06/2009	Sheet of
File:	G:\ESTUDIOS\..BIOamp.SchDoc	Drawn By:



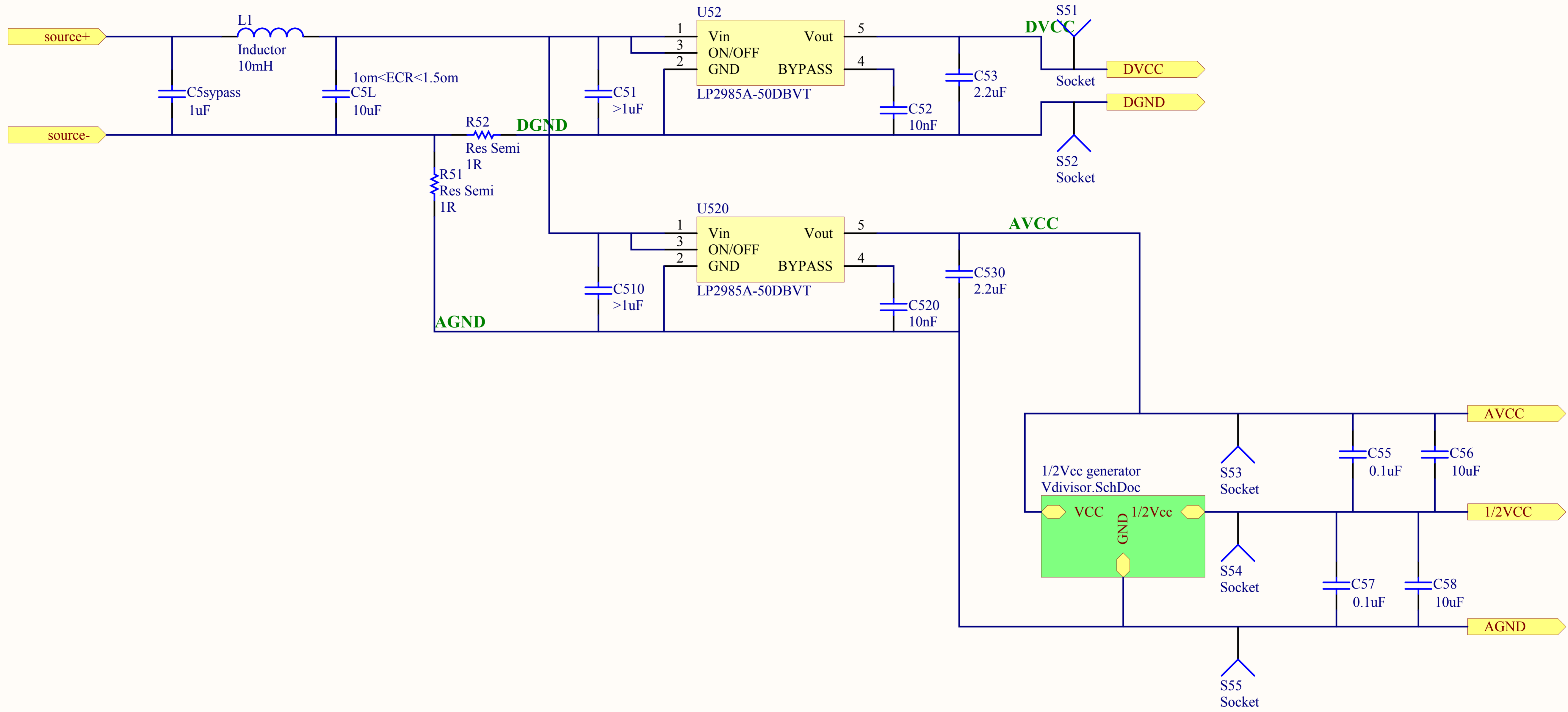
Title		
Size	Number	Revision
A3		
Date:	11/06/2009	Sheet of
File:	G:\ESTUDIOS\current_isolated.SchDoc	Drawn By:

Transconductance = 0.5 mA/V

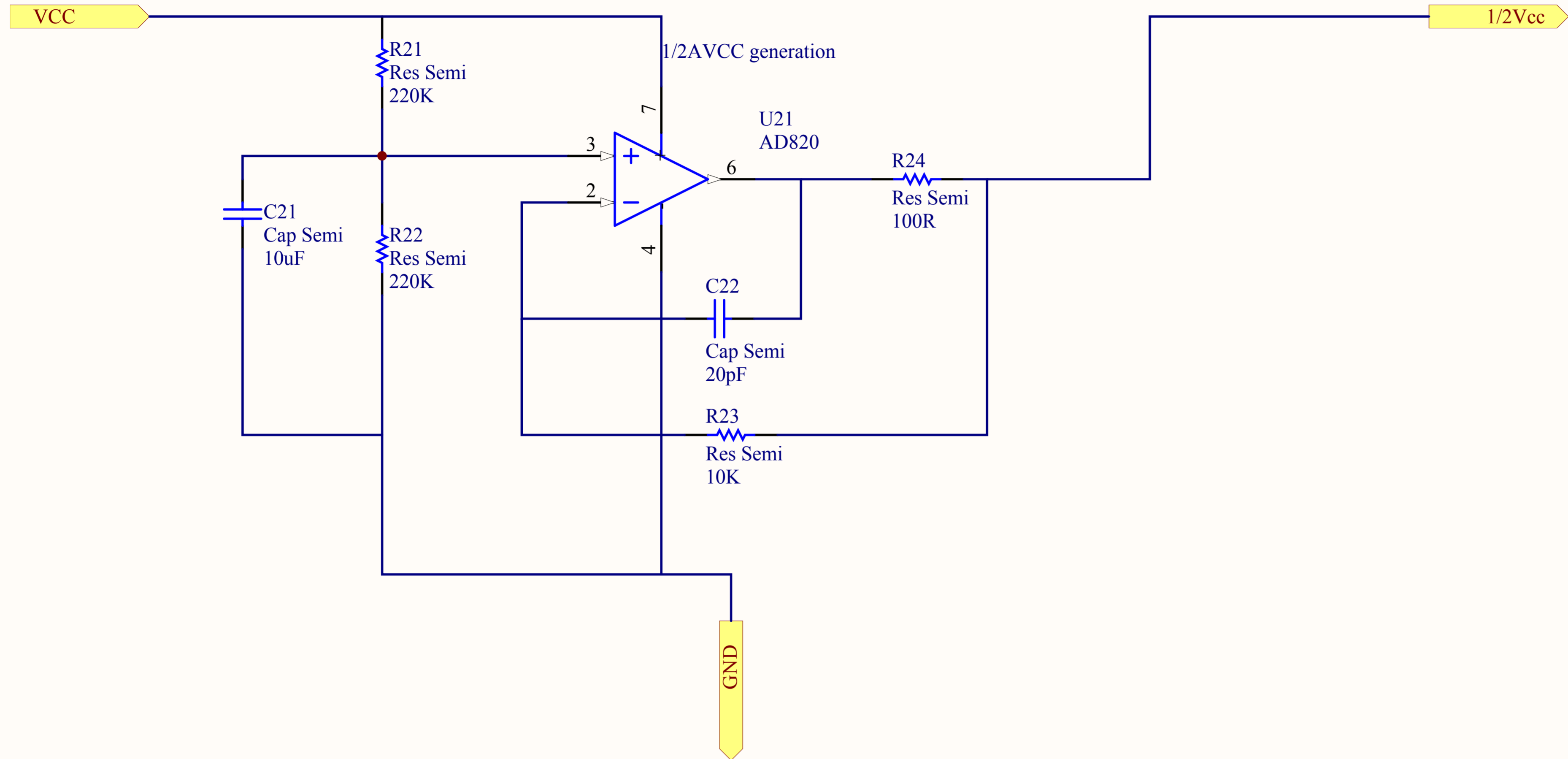
DC rejection filter (f<12Hz) DC rejection filter (f<112Hz)



Title		
Size	Number	Revision
A4		
Date:	11/06/2009	Sheet of
File:	G:\ESTUDIOS\..current_injection.SchDoc Drawn By:	



Title		
Size	Number	Revision
A4		
Date:	11/06/2009	Sheet of
File:	G:\ESTUDIOS\...\power+clk.SchDoc	Drawn By:



Title		
Size	Number	Revision
A4		
Date:	11/06/2009	Sheet of
File:	G:\ESTUDIOS\...\Vdivisor.SchDoc	Drawn By: